SEMARAK ILMU PUBLISHING

CFD Letters

Journal homepage:
https://semarakilmu.com.my/journals/index.php/CFD_Letters/index
ISSN: 2180-1363

Impact of Variable Fluid Properties on the Peristaltic Flow of Eyring-powell Fluid through Porous Medium: Applications to Hemodynamics

Prathiksha[1], Manjunatha Gudekote[1,*], Rajashekhar Choudhari[2], Hanumesh Vaidya[3], Kerehalli Vinayaka Prasad[3]

[1] Department of Mathematics, Manipal Institute of Technology, Manipal Academy of Higher Education, Manipal, India
[2] Department of Mathematics, Manipal Institute of Technology Bengaluru, Manipal Academy of Higher Education, Manipal, India
[3] Department of Mathematics, Vijayanagara Sri Krishnadevaraya University, Ballari, Karnataka, India

ARTICLE INFO

Article history:
Received 5 February 2024
Received in revised form 8 March 2024
Accepted 10 April 2024
Available online 31 August 2024

Keywords:
Eyring-Powell Fluid; Varying Viscosity; Perturbation Technique; Darcy Number

ABSTRACT

The main focus of this study is to examine the peristaltic behaviour of an Eyring-Powell fluid within a non-uniform porous channel. The investigation focuses on comprehending the characteristics of the channel walls that impact the fluid dynamics. By incorporating the convective boundary conditions into the series Perturbation method, solutions for the governing non-linear equations on velocity, temperature, and stream function are obtained. The study improves accessibility through parametric assessment, and the results are shown graphically using MATLAB R2023a software. Significant insights are obtained from the study, especially concerning natural phenomena such as blood flow in tiny arteries, which may be used for management or intervention in dysfunctional situations. The investigation results show that fluid characteristics are greatly affected by porous parameters and different viscosities. Also, fluid flow improves as the porous parameter increases, i.e., Darcy number. The enhancement in the convective heat and mass transfer coefficient decreases the temperature and concentration of the fluid, respectively.

1. Introduction

Peristalsis is a physiological phenomenon characterised by the rhythmic contraction and relaxation of muscles within tubular structures, such as the oesophagus, digestive tract, and particular blood vessels. The organised wave-like movement in these tubes moves things along, which helps with digestion and blood flow. Peristalsis is a biological mechanism that is exclusive to living organisms. In biological systems, the peristaltic mechanism is the transmission of muscle contractions in wave-like patterns. These waves move the content forward by applying a propulsive force to travel longitudinally through tubular structures. Streamline processes, such as the transportation of food through the digestive tract, are achieved by ensuring unidirectional flow and smooth coordination of the material in the medium flow. Ayukawa and Takabatake [1] investigated the patterns of peristaltic flow in a two-dimensional setting. Siddiqui and Schwarz [2] explored the

* *Corresponding author.*
E-mail address: manjunatha.g@manipal.edu (Manjunatha Gudekote)

https://doi.org/10.37934/cfdl.17.1.114139

peristaltic motion of second-order fluids, which yielded crucial knowledge regarding the flow. Comparini and Mannucci [3] investigated the interplay between Bingham and Newtonian fluids. Based on their work, critical observations were made on the behaviour of different fluid types in peristaltic systems. Elshehawey *et al.,* [4] studied the peristalsis of generalized Newtonian fluid in a porous medium by considering so slip boundary condition. Further peristaltic fluxes were examined by Hayat *et al.,* [5] through the application of magnetohydrodynamics (MHD) on the behaviour of Johnson-Segalman fluid. The effect of heat transfer, slip circumstances, and wall characteristics on MHD peristaltic transport was examined by Srinivas *et al.,* [6]. The aim was to investigate the pragmatic consequences of these variables in actual circumstances.

Material porosity is the ratio of its vacant spaces, or pores, to its overall volume. The porosity parameter controls fluid flow, heat transfer, and transport phenomena in porous media, including rocks, soils and artificial materials. The intrinsic void volume in the material is known as Porosity. The capacity of a medium to facilitate fluid transmission is heavily influenced by its porosity. Further, the effect of porosity on heat transfer within the porous medium is critical. This is important for geothermal reservoirs and heat exchangers. Porous medium/porosity affects many scientific, technical, and environmental fields. Porosity characterisation and understanding are essential for accurate prediction and efficient optimisation of fluid flow, heat transfer, and mass transport in porous materials. Ramesh and Devakar [7] studied the MHD peristaltic transport characteristics of fluids exhibiting couple-stress properties across porous media. The study examined inclined asymmetric channels and heat conduction, which is relevant to the industry. Sankad and Nagathan [8] led a research investigation to augment knowledge regarding unsteady MHD peristaltic flows of fluids in porous media, emphasising fluids exhibiting a couple of stress characteristics. Gudekote and Choudhari [9] conducted a study investigating the impact of slip effects on the peristaltic transport of Casson fluids within inclined elastic tubes featuring porous walls. Peristaltic slip flow in inclined porous conduits was investigated in the research conducted by Lakshminarayana *et al.,* [10], with a particular emphasis on Bingham fluids. This research possesses substantial pertinence about industrial applications. Further heat and mass transport in MHD peristaltic fluxes through compliant porous channels were investigated in the study reported by Vaidya *et al.,* [11] and Tanveer *et al.,* [12] by considering convective boundary. Abuiyada *et al.,* [13] examined the impact of activation energy and chemical reaction on the MHD peristaltic flow of Jeffery nanofluids through a porous medium in an inclined symmetric channel. The effects of diffusion thermography, Joule heating, radiation, viscous dissipation, heat generation/absorption, activation energy, and thermal diffusion are also investigated.

Muscles contract and relax during peristalsis to move substances in tubular structures. Variable fluid parameters, such as viscosity and thermal conductivity, impact the process. Viscosity measures the fluid's flow resistance. Variable viscosity is a liquid's capacity to change flow resistance under different conditions. A rise in viscosity amplifies the resistance of fluids during peristaltic motion, which may necessitate additional exertion to propel liquids through a conduit. Varying viscosity slows peristaltic waves and reduces peristalsis. To comprehend peristalsis, the relationship between stress, strain rate, and viscosity is critical in non-Newtonian fluids. Material thermal conductivity impacts heat production during peristalsis. Muscle contractions modify energy transfer and thermal conductivity within the conduit. Variable thermal conductivity affects fluid and tissue temperature distribution, which may affect peristalsis-related physiological systems also affects peristalsis fluid interactions, biomechanics, energy consumption, heat production, and fluid transmission efficiency. These changes affect gastrointestinal and biomechanics. The investigations conducted previously by Pascal *et al.,* [14], Lathif *et al.,* [15], Khan *et al.,* [16,17], Gudekote *et al.,* [18], Khan *et al.,* [19], Prasad *et al.,* [20] and Mukhopadhyay *et al.,* [21] covers various aspects of fluid flow, including heat transfer

with variable fluid properties. These studies provide significant contributions to the understanding of these intricate phenomena. The investigators undertook an in-depth examination to determine the effect of various liquid properties on this phenomenon.

Fluid heat transmission is crucial for natural and artificial phenomena. The primary heat transmission mechanisms are conduction, convection, and radiation. Solids exhibit more conductivity than fluids due to higher intermolecular spacing. Conduction occurs in fluids with temperature gradients. Heat transfer by fluid motion, such as liquids and gases, is called Convection. Radiation is the transmission of heat via electromagnetic waves. Contrary to conduction and convection, this heat transfer method operates based on the temperature difference between the fluid and its environment. The heat conductivity of the liquid has a significant impact on the process. Peristalsis, which promotes blood flow and nutrient absorption, may increase heat transmission between blood and tissues and affect local temperature conditions in the digestive system. Scholars analyse peristalsis-related heat transport through computational simulations and mathematical models. By identifying heat-generating processes and forecasting temperature fluctuations, these models aid in comprehending the thermal impacts on peristaltic motion. Although peristalsis does not involve direct heat transfer, physiological processes, therapeutic applications, and biomechanical research must understand its heat-related aspects. Vajravelu *et al.,* [22] investigated the influence of heat transmission on the peristaltic transport of a Jeffrey fluid through a porous stratum oriented vertically. This work expands the understanding of the uses of porous media. Alarabi *et al.,* [23] explored the heat transfer phenomena in the peristaltic flow of viscoelastic fluid within eccentric cylinders using the homotopy perturbation approach. Dar and Elangovan [24] studied the effect of an angled magnetic field on heat and mass transfer in the peristaltic flow of stress fluids. The investigation adds to the existing corpus of information about magnetic effects in this particular setting. A study was undertaken by Abdulhadi and Ahmed [25] to examine the impact of radial magnetic fields on the peristaltic transport of a Jeffrey fluid through curved channels. The investigation has produced noteworthy results concerning the possible application of magnetic fields in peristalsis. Khan *et al.,* [26] analysed Williamson nanofluid's heat and mass transfer by considering the effects of variable viscosity and inclined Lorentz force over a stretching sheet. Magesh and Kothandapani [27] examined heat and mass transfer in non-Newtonian fluid motion caused by peristaltic pumping in asymmetrically curved channels. The study analysed the significance of non-Newtonian behaviours in curved geometries. Vaidya *et al.,* [28] conducted more studies to evaluate peristaltic transport. The study emphasises the importance of heat transport and slide effects in an axisymmetric porous tube.

The linear relationship between attrition stress and average velocity in neutronic fluids deviates from that observed in Eyring-Powell rheology. In this fluid model, the Powell-Eyring and Eyring rheological models are implemented. The non-Newtonian nature of Eyring-Powell fluid causes its viscosity to vary in response to changes in flow rate. Eyring-Powell fluid and other non-Newtonian liquids characterise their flow, adhesion, and dispersion by their densities. Flow velocity, conversely, determines the thickness of Newtonian fluids. The Eyring model is elucidated through the application of quantum chemistry. According to this idea, liquid particles are structurally organised. The destruction or repairs of these structures affect the deposit. A corrective term is incorporated into the Powell-Eyring component to accommodate viscoelastic effects. This segment improves the representation of liquid behaviour, specifically in cases where accelerations deviate substantially from the reference acceleration. The Eyring-Powell fluid model applies to biomechanics, chemistry, and fluid dynamics. This is the common term for the movement of complex fluids, such as those found in biological systems, industrial processes, and polymers. The consistency index, reference twisting index, and activation energy are all components of Eyring-Powell fluid numbers. Predicting

the rheological parameters of the Eyring-Powell fluid under different flow conditions is of the utmost importance. Engineers and researchers employ this model to investigate the properties of non-Newtonian fluids and improve processes that incorporate them. Adapting the Eyring-Powell fluid model in the study becomes crucial as it facilitates investigating intricate rheological characteristics of various substances. Many researchers have carried out studies on the Eyring-Powell fluid as seen in the literature [29-39].

Further research is necessary to comprehend the collective influence of various factors on Eyring-Powell fluid peristaltic transport. It is crucial to comprehend the relative significance of different elements to derive practical implications and adapt the Eyring-Powell fluid model to accommodate physiological investigations. To fill this void, the present work explores heat transfer in a non-uniform channel with convective boundary conditions during the peristalsis of Eyring-Powell fluid in a porous media. To comprehend the relationship between the permeability of the medium and its surroundings, which affects biological processes, including nutrient distribution and spatial temperature within the porous medium, it is vital to account for convective heat exchange at channel boundaries. The present investigation is utilised in drug transport model delivery optimisation to examine the impact of temperature on the dispersion of medications in porous media.

2. Mathematical Formulations

The problem is quantitatively described using the continuity, momentum, temperature, and concentration equations, which are the fundamental equations of fluid dynamics. Consider the flow of viscous incompressible Eyring-Powell fluid through a non-uniform two-dimensional channel.

The wall deformation expression for the geometry of the channel is given as,

$$H'(x',t') = a'(x') + b'\,sin\left[\frac{2\pi}{\lambda}(x' - ct')\right] \tag{1}$$

Where H' is the non-uniform wave in which t' is the time, $a'(x') = a' + m'x'$ with $m' \ll 1$ which represent the channels half-width at any axial distance x' , a' is the non-uniform radius, m' is the constant depending on the length of the channel, c is the wave speed, λ is the wave length and b' is the wave amplitude. Figure 1 shows geometry of the physical model.

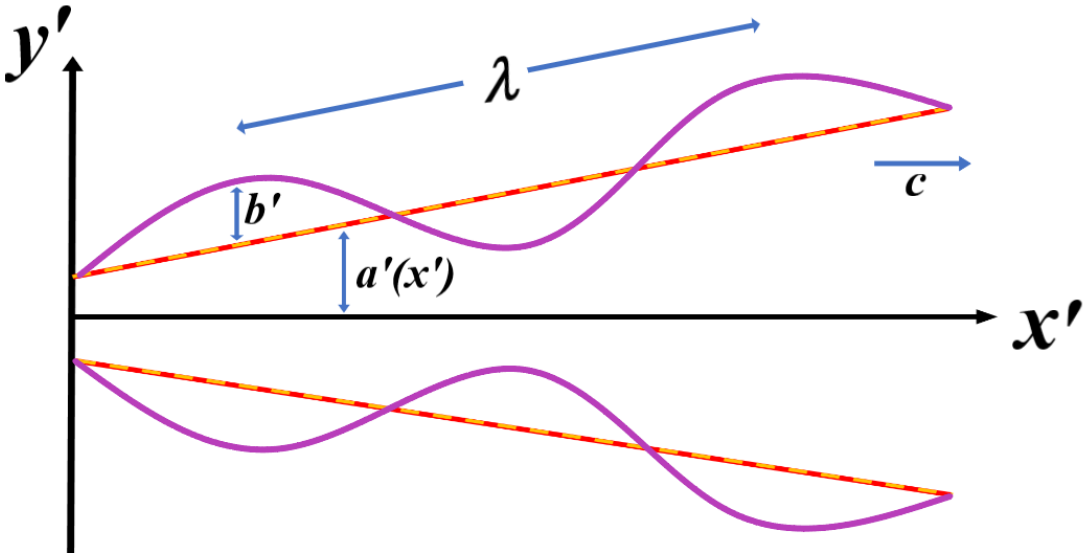

Fig. 1. Geometry of the physical model

The Eyring-Powell fluid model is used to explore non-Newtonian flow shear. In the Eyring–Powell fluid model, the stress tensor is defined by Akbar [30] as follows:

$$S' = \mu \nabla V + \frac{1}{\beta_1} \sinh^{-1}\left[\frac{1}{c_1}\nabla V\right] \tag{2}$$

$$\sinh^{-1}\left[\frac{1}{c_1}\nabla V\right] \cong \frac{1}{c_1}\nabla V - \frac{1}{6}\left(\frac{1}{c_1}\nabla V\right)^3 , \left|\frac{1}{c_1}\nabla V\right|^5 \ll 1, \tag{3}$$

Where μ is related to the shear viscosity measurement, β_1 and c_1 account for the fluid model representatives. ∇ is the vector differential operator and V is the velocity component.

2.1 Governing Equations

For the fluid flowing in the fixed frame, the incompressibility conditions for the governing equation are given as,

Continuity equation:

$$\frac{\partial \hat{v}}{\partial x'} + \frac{\partial \hat{w}}{\partial y'} = 0 \tag{4}$$

Momentum equation:

$$\rho\left[\frac{\partial \hat{w}}{\partial t'} + \hat{w}\,\frac{\partial \hat{w}}{\partial x'} + \hat{v}\frac{\partial \hat{w}}{\partial y'}\right] = -\frac{\partial p'}{\partial x'} + \frac{\partial S'_{x'x'}}{\partial x'} + \frac{\partial S'_{x'y'}}{\partial y'} - \frac{\mu}{k}(\hat{w} + c) \tag{5}$$

$$\rho\left[\frac{\partial \hat{v}}{\partial t'} + \hat{w}\frac{\partial \hat{v}}{\partial x'} + \hat{v}\frac{\partial \hat{v}}{\partial y'}\right] = -\frac{\partial p'}{\partial y'} + \frac{\partial S'_{x'y'}}{\partial x'} + \frac{\partial S'_{y'y'}}{\partial y'} \tag{6}$$

Energy equation:

$$\rho C_P\left[\frac{\partial T'}{\partial t'} + \hat{v}\frac{\partial T'}{\partial x'} + \hat{w}\frac{\partial T'}{\partial y'}\right] = \frac{\partial}{\partial x'}\left(K(T')\frac{\partial T'}{\partial x'}\right) + \frac{\partial}{\partial y'}\left(K(T')\frac{\partial T'}{\partial y'}\right) + S'_{x'x'}\,\frac{\partial \hat{v}}{\partial x'} + S'_{y'y'}\,\frac{\partial \hat{w}}{\partial y'} + S'_{x'y'}\left(\frac{\partial \hat{w}}{\partial y'} + \frac{\partial \hat{v}}{\partial x'}\right) \tag{7}$$

Concentration equation:

$$\left[\frac{\partial C'}{\partial t'} + \hat{v}\frac{\partial C'}{\partial x'} + \hat{w}\frac{\partial C'}{\partial y'}\right] = D_m\left[\frac{\partial^2 C'}{\partial x'^2} + \frac{\partial^2 C'}{\partial y'^2}\right] + \frac{D_m K_T}{T_m}\left[\frac{\partial^2 T'}{\partial x'^2} + \frac{\partial^2 T'}{\partial y'^2}\right] \tag{8}$$

Where $\hat{v}$, $\hat{w}$ are velocity components in axial and radial directions of the fixed frame respectively. p' is the pressure, ρ is the fluid density, $S'_{x'x'}$, $S'_{x'y'}$, $S'_{y'y'}$ are extra stress components, while T' denotes temperature, C' denotes concentration, C_P denotes the specific heat at constant volume and $K(T')$ denotes variable thermal conductivity, T_m the mean temperature, D_m the coefficient of mass diffusivity, and K_T the thermal diffusion ratio.

The above-mentioned dimensional parameters are non-dimensionalised using the following.

$$x = \frac{x'}{\lambda}, y = \frac{y'}{a'}, \ w = \frac{\hat{w}}{c}, \ v = \frac{\lambda \hat{v}}{c a'}, S_{xx} = \frac{a' S'_{x'x'}}{c\,\mu}, S_{xy} = \frac{a' S'_{x'y'}}{c\,\mu}, S_{yy} = \frac{a' S'_{y'y'}}{c\,\mu}, t = \frac{c\,t'}{\lambda},$$
$$Re = \frac{a\,c\,\rho}{\mu}, \ \vartheta = \frac{\mu_0}{\rho}, \ p = \frac{a'^2 p'}{c\,\lambda\,\mu}, \theta = \frac{T' - T'_0}{T_1 - T_0}, Pr = \frac{\mu\, C_P}{k_1}\, Ec = \frac{c^2}{\delta T_0}, Br = Ec\, Pr, \delta = \frac{a'}{\lambda}$$
$$\phi = \frac{C' - C'_0}{C'_0}, \mu'_0 = \frac{\mu_0}{\mu}, \ Sr = \frac{\rho D_m K_T (T' - T'_0)}{T_m C'_0}, \ Sc = \frac{\mu}{\rho D_m}, Da = \frac{k}{a'^2\,\mu}, B = \frac{1}{\mu \beta_1 c_1}, A = \frac{Bc^2}{2\,a'^2 c_1^2},$$
$$E_1 = -\frac{\tau a'^3}{\lambda \mu_0^3 c'}, \ E_2 = \frac{m_1\, a'^3 c}{\lambda^3 \mu_0}, E_3 = \frac{m_2 a'^3}{\lambda^2 \mu_0}, E_4 = \frac{m_3 a'^3}{\lambda^5 \mu_0 c}, \ E_5 = \frac{H' a'^3}{\lambda \mu_0\, c}, \epsilon = \frac{b'}{a'}, \ \psi = \frac{\psi'}{a' c},$$
$$B_h = \frac{h_1 a'}{k}, B_m = \frac{h_2 a'}{D_m}, h = \frac{H'}{a'} = 1 + mx + \epsilon \sin\big(2\pi(x - t)\big) \tag{9}$$

Where, E_1 is Wall tension parameter, E_2 is Mass characterization parameter, E_3 is Wall damping force parameter, E_4 is Wall rigidity parameter, E_5 is Wall elasticity parameter, Sc is Schmidt number, Sr is Soret number, Br is Brinkman number, B_h is Convective Heat Transfer Coefficient, B_m is Convective Mass Transfer Coefficient, A is Eyring–Powell fluid parameter, B is Eyring–Powell fluid material parameter, Da is Darcy Number, β is Velocity slip parameter, ϵ is Amplitude ratio, α is Coefficient of Variable Viscosity, ν is Coefficient of Variable thermal conductivity, m is non-uniform parameter, t is time, x is non-dimensional axial distance, Pr is Prandlt number, Ec is Ecart number, Re is Reynolds number, δ is wave number.

The governing equations can be expressed in a non-dimensional form by utilizing the quantities provided in Eq. (9) as,

$$\delta \frac{\partial v}{\partial x} + \frac{\partial w}{\partial y} = 0 \tag{10}$$

$$Re \left[\delta v \frac{\partial w}{\partial x} + w \frac{\partial w}{\partial y}\right] = -\frac{\partial p}{\partial x} + \delta \frac{\partial S_{xx}}{\partial x} + \frac{\partial S_{xy}}{\partial y} - \frac{1}{Da}(w + 1) \tag{11}$$

$$Re\, \delta \left[\delta v \frac{\partial v}{\partial x} + w \frac{\partial v}{\partial y}\right] = -\frac{\partial p}{\partial y} + \delta^2 \frac{\partial S_{xy}}{\partial x} + \delta \frac{\partial S_{yy}}{\partial y} \tag{12}$$

$$Re\, \delta \left[\delta v \frac{\partial \theta}{\partial x} + w \frac{\partial \theta}{\partial y}\right] = Ec \left[\left(\delta S_{xx} \frac{\partial w}{\partial x} + S_{yy} \frac{\partial v}{\partial y}\right) + S_{xy}\left(\delta \frac{\partial v}{\partial x} + \frac{\partial w}{\partial y}\right)\right] + \frac{1}{Pr}\left[\delta^2 \frac{\partial}{\partial x}\left(K(\theta)\frac{\partial \theta}{\partial x}\right) + \frac{\partial}{\partial y}\left(K(\theta)\frac{\partial \theta}{\partial y}\right)\right] \tag{13}$$

$$Re \left[\delta\, v \frac{\partial \sigma}{\partial x} + w \frac{\partial \sigma}{\partial y}\right] = \frac{1}{Sc}\left[\delta^2 \frac{\partial^2 \sigma}{\partial x^2} + \frac{\partial^2 \sigma}{\partial y^2}\right] + Sr \left[\delta^2 \frac{\partial^2 \theta}{\partial x^2} + \frac{\partial^2 \theta}{\partial y^2}\right] \tag{14}$$

Introducing the dimensionless stream function ψ using $w = \frac{\partial \psi}{\partial y}$ and $v = -\delta \frac{\partial \psi}{\partial y}$ and by implementing long wavelength and small Reynolds number assumptions, Eq. (10) to Eq. (14) takes the form.

$$\frac{\partial p}{\partial x} = \frac{\partial S_{xy}}{\partial y} - \frac{1}{Da}\left(\frac{\partial \psi}{\partial y} + 1\right) \tag{15}$$

$$\frac{\partial p}{\partial y} = 0 \tag{16}$$

$$\frac{\partial}{\partial y}\left\{k(\theta)\frac{\partial \theta}{\partial y}\right\} + Br\, S_{xy} \frac{\partial^2 \psi}{\partial y^2} = 0 \tag{17}$$

$$\frac{\partial^2 \sigma}{\partial y^2} + ScSr\frac{\partial^2 \theta}{\partial y^2} = 0 \tag{18}$$

S_{xy} gives the constitutive equation of Eyring-Powell fluid as

$$S_{xy} = \{\mu(y) + B\}\frac{\partial^2 \psi}{\partial y^2} - \frac{A}{3}\left(\frac{\partial^2 \psi}{\partial y^2}\right)^3 \tag{19}$$

2.2 Boundary Conditions

Peristalsis refers to the dynamic interplay between a fluid medium (such as blood or digestive liquids) and the structure of a biological conduit (such as the intestines or blood vessels). The fluid's interaction with the channel walls is governed by boundary conditions, which take slip, viscosity, and the physical properties of the walls into account. Peristalsis is a process that incorporates not just fluid dynamics but also the transfer of mass and heat. Temperature, concentration, and other pertinent boundary conditions are essential for simulating these transfer events within the biological conduit. It is imperative to comprehend boundary conditions' impact on therapeutic applications. It provides treatment planning and medical diagnosis with information regarding the potential effects of conduit wall characteristics or changes in physiological parameters on peristaltic motion.

Let $y' = 0$ be the lowest static wall for the porous channel. The top wavy wall of the permeable channel and the interfacial wavy area are represented by $y' = H'(x,t)$.

Let the porous boundary conditions imposed on the lower and upper walls be given as:

$$\frac{\partial \hat{w}}{\partial y'} = 0 \text{ at } y' = 0 \text{ and } -\frac{\sqrt{k}}{b'}S'_{x'y'} = -(\hat{w} + c) \text{ at } y' = H'(x,t) \tag{20}$$

Convective heat exchange occurring at upper and lower isothermal walls of the channel is given by:

$$\frac{\partial T'}{\partial y'} = 0 \text{ at } y' = 0 \text{ and } -k\frac{\partial T'}{\partial y'} = h_1(T' - T'_0) \text{ at } y' = H'(x,t) \tag{21}$$

The concentration profile at the lower static wall and upper wall of the porous channel is governed by the following conditions:

$$\frac{\partial C'}{\partial y'} = 0 \text{ at } y' = 0 \text{ and } -D\frac{\partial C'}{\partial y'} = h_2(C' - C'_0) \text{ at } y' = H'(x,t) \tag{22}$$

Porous and convective conditions must be employed to mimic and optimise various technical and natural systems, including heat transmission, filtration, environmental studies, and biological systems. Chemical reactors, energy systems, food processing, and bioreactors require convective boundary conditions to model and improve ecological restoration.

Introducing the dimensionless stream function ψ using $v = \frac{\partial \psi}{\partial y}$ and $w = -\delta\frac{\partial \psi}{\partial y}$ and by implementing long wavelength and small Reynolds number assumptions to equations, the non-dimensional convective boundary conditions are given by,

$$\frac{\partial^2 \psi}{\partial y^2} = 0\,,\ \frac{\partial \theta}{\partial y} = 0\,,\frac{\partial \phi}{\partial y} = 0 \ \ at\ \ y = 0 \tag{23}$$

$$\frac{\partial \psi}{\partial y} + \frac{\sqrt{Da}}{\beta} S_{xy} = -1 \, , B_h \theta + \frac{\partial \theta}{\partial y} = 0 \, , B_m \phi + \frac{\partial \phi}{\partial y} = 0 \quad \text{at } y = h \tag{24}$$

Further $\mu(y)$ and $k(\theta)$ are the variable viscosity and thermal conductivity which are considered as a function of y and θ and is given by,

$$\mu(y) = e^{-\alpha y} = 1 - \alpha y + O(\alpha^2) \tag{25}$$

$$k(\theta) = e^{\nu \theta} = 1 + \nu \theta + O(\nu^2) \tag{26}$$

3. Solution Methodology: Perturbation Technique

The mathematical formulation introduced in the preceding section is solved in this section. Due to the nonlinear nature of the system, it is impossible to derive a closed-form solution. The formulas for streamlines and temperature are instead derived using a perturbation approach, emphasising low values of the Eyring-Powell fluid parameter A. Thus, the following solution is considered.

$$\psi = \psi_0 + A \, \psi_1 + O(A^2) \tag{27a}$$

$$\theta = \theta_0 + A \, \theta_1 + O(A^2) \tag{27b}$$

By ignoring $O(A^2)$, Zeroth and First order system of equations are obtained.

Equation for streamlines of zeroth order is given by

$$\left(P + \frac{1}{Da}\right) y + \frac{1}{Da} \psi_0 = \{1 - \alpha \, y + B\} \frac{\partial^2 \psi_0}{\partial y^2} \tag{28}$$

With boundary conditions

$$\frac{\partial^2 \psi_0}{\partial y^2} = 0 \quad at \quad y = 0 \ and \quad \frac{\partial \psi_0}{\partial y} + \frac{\sqrt{Da}}{\beta} (1 - \alpha \, y + B) \frac{\partial^2 \psi_0}{\partial y^2} = -1 \quad at \quad y = h \tag{29}$$

Equation for streamlines of first order is given by

$$(1 - \alpha \, y + B) \frac{\partial^2 \psi_1}{\partial y^2} - \frac{1}{Da} \psi_1 - \frac{1}{3} \left(\frac{\partial^2 \psi_0}{\partial y^2}\right)^3 = 0 \tag{30}$$

With boundary conditions

$$\frac{\partial^2 \psi_1}{\partial y^2} = 0 \ at \ y = 0 \ and \ \frac{\partial \psi_1}{\partial y} + \frac{\sqrt{Da}}{\beta} \left\{ (1 - \alpha \, y + B) \frac{\partial^2 \psi_1}{\partial y^2} - \frac{1}{3} \left(\frac{\partial^2 \psi_0}{\partial y^2}\right)^3 \right\} = 0 \ at \ y = h \tag{31}$$

Equation for temperature of zeroth order is given by

$$\frac{\partial \theta_0}{\partial y} + \nu \, \theta_0 \frac{\partial \theta_0}{\partial y} + \int Br \left\{ (1 - \alpha \, y + B) \left(\frac{\partial^2 \psi_0}{\partial y^2}\right)^2 \right\} \partial y = 0 \tag{32}$$

With boundary conditions

$$\frac{\partial \theta_0}{\partial y} = 0 \quad \text{at} \quad y = 0 \quad \text{and} \quad B_h \theta_0 + \frac{\partial \theta_0}{\partial y} = 1 \text{ at } y = h \tag{33}$$

Equation for temperature of first order is given by

$$\frac{\partial \theta_1}{\partial y} + \nu\, \theta_0 \frac{\partial \theta_1}{\partial y} + \nu\, \theta_1 \frac{\partial \theta_0}{\partial y} + \int Br \left\{ 2(1 - \alpha\, y + B) \left(\frac{\partial^2 \psi_0}{\partial y^2}\right)\left(\frac{\partial^2 \psi_1}{\partial y^2}\right) - \frac{1}{3}\left(\frac{\partial^2 \psi_0}{\partial y^2}\right)^4 \right\} \partial y = 0 \tag{34}$$

With boundary conditions

$$\frac{\partial \theta_1}{\partial y} = 0 \quad \text{at} \quad y = 0 \quad \text{and} \quad B_h\, \theta_1 + \frac{\partial \theta_1}{\partial y} = 0 \quad \text{at} \quad y = h \tag{35}$$

Since the equations are non-linear, the double perturbation approach is employed to find the solutions.

$$\psi_i = \Sigma \alpha^j \psi_{ij} \text{ , where } 0 \le j \le n \text{ , } i = \{0,1\} \tag{36}$$

$$\theta_i = \Sigma\, \nu^j\ \theta_{ij} \text{ , where } 0 \le j \le n \text{ , } i = \{0,1\} \tag{37}$$

Higher order terms are disregarded to simplify solutions for streamlines and temperature, i.e., $O(\alpha_1^2)\ and\ O(\alpha_2^2)$. The resulting streamline and temperature equations are as follows.

$$\psi_0 = \psi_{00} + \alpha\, \psi_{01} \tag{38a}$$

$$\psi_1 = \psi_{10} + \alpha\, \psi_{11} \tag{38b}$$

$$\theta_0 = \theta_{00} + \nu\, \theta_{01} \tag{39a}$$

$$\theta_1 = \theta_{10} + \nu\, \theta_{11} \tag{39b}$$

Substituting Eq. (38a) in Eq. (28) and Eq. (29),

The equation for zeroth order stream function, along with porous boundary conditions, is derived as

$$\frac{\partial^2 \psi_{00}}{\partial y^2} - \frac{1}{Da(1+B)} \psi_{00} = \frac{\left(P - \frac{1}{Da}\right)}{(1+B)} y$$

$$\frac{\partial^2 \psi_{00}}{\partial y^2} = 0 \quad \text{at} \quad y = 0 \text{ and } \quad \frac{\partial \psi_{00}}{\partial y} + \frac{\sqrt{Da}}{\beta}(1 + B) \frac{\partial^2 \psi_{00}}{\partial y^2} = -1 \quad \text{at} \quad y = h \tag{40}$$

The equation for first order stream function along with porous boundary conditions is derived as

$$\frac{\partial^2 \psi_{01}}{\partial y^2} - \frac{1}{Da(1+B)} \psi_{01} = y\, \frac{\partial^2 \psi_{00}}{\partial y^2}$$

$$\frac{\partial^2 \psi_{01}}{\partial y^2} = 0 \quad \text{at} \quad y = 0 \text{ and } \frac{\partial \psi_{01}}{\partial y} + \frac{\sqrt{Da}}{\beta}\, (1 + B) \frac{\partial^2 \psi_{01}}{\partial y^2} + \beta_1 y\, \frac{\partial^2 \psi_{00}}{\partial y^2} = 0 \quad \text{at } y = h \tag{41}$$

Substituting Eq. (38b) in Eq. (30) and Eq. (31),

The equation for zeroth order stream function, along with porous boundary conditions, is derived as

$$\frac{\partial^2\psi_{10}}{\partial y^2} - \frac{1}{Da(1+B)}\psi_{10} = \frac{1}{3(1+B)}\left(\frac{\partial^2\psi_{00}}{\partial y^2}\right)^3$$

$$\frac{\partial^2\psi_{10}}{\partial y^2} = 0 \;\text{ at }\; y = 0 \;\text{ and }\; \frac{\partial\psi_{10}}{\partial y} + \frac{\sqrt{Da}}{\beta}\left\{(1+B)\,\frac{\partial^2\psi_{10}}{\partial y^2} - \frac{1}{3}\left(\frac{\partial^2\psi_{00}}{\partial y^2}\right)^3\right\} = 0 \;\text{ at }\; y = h \tag{42}$$

The equation for first order stream function along with porous boundary conditions is derived as

$$\frac{\partial^2\psi_{11}}{\partial y^2} - \frac{1}{Da(1+B)}\psi_{11} = \frac{1}{(1+B)}\left[y\,\frac{\partial^2\psi_{10}}{\partial y^2} + \left(\frac{\partial^2\psi_{00}}{\partial y^2}\right)^2\left(\frac{\partial^2\psi_{10}}{\partial y^2}\right)\right]$$

$$\frac{\partial^2\psi_{11}}{\partial y^2} = 0 \text{ at } y = 0 \text{ and } \frac{\partial\psi_{11}}{\partial y} + \frac{\sqrt{Da}}{\beta}\left\{(1+B)\,\frac{\partial^2\psi_1}{\partial y^2} - y\,\frac{\partial^2\psi_{10}}{\partial y^2} - \left(\frac{\partial^2\psi_{00}}{\partial y^2}\right)^2\left(\frac{\partial^2\psi_{10}}{\partial y^2}\right)\right\} = 0 \text{ at } y = h \tag{43}$$

Combining the solved equations, i.e., Eq. (40) - Eq. (43) with corresponding boundary conditions, the expression for stream function is obtained as,

$$\psi = \psi_{00} + \alpha\,\psi_{01} + A\,\psi_{10} + A\,\alpha\,\psi_{11} \tag{44}$$

Utilising equation $w = \frac{\partial\psi}{\partial y}$, solution for velocity is obtained.

Similarly, on using Eq. (39a) in Eq. (32) and Eq. (33). The equation for the zeroth order temperature expression along with convective boundary conditions is derived as

$$\frac{\partial\theta_{00}}{\partial y} + \int Br\;\left\{(1-\alpha y+B)\left(\frac{\partial^2\psi_0}{\partial y^2}\right)^2\right\}\partial y\; = 0$$

$$\frac{\partial\theta_{00}}{\partial y} = 0 \;\text{ at }\; y = 0 \;\text{ and }\; B_h\theta_{00} + \frac{\partial\theta_{00}}{\partial y} = 1 \;\text{ at }\; y = h \tag{45}$$

The equation for the first order temperature expression along with convective boundary conditions is derived as

$$\frac{\partial\theta_{01}}{\partial y} + \theta_{00}\frac{\partial\theta_{00}}{\partial y} = 0$$

$$\frac{\partial\theta_{01}}{\partial y} = 0 \;\text{ at }\; y = 0 \;\text{ and }\; B_h\,\theta_{01} + \frac{\partial\theta_{01}}{\partial y} = 0 \;\text{ at }\; y = h \tag{46}$$

Substituting Eq. (39b) in Eq. (34) and Eq. (35),

The equation for the zeroth order temperature expression along with convective boundary conditions is derived as

$$\frac{\partial\theta_{10}}{\partial y} + \int Br\;\left\{2(1-\alpha\,y+B)\left(\frac{\partial^2\psi_0}{\partial y^2}\right)\left(\frac{\partial^2\psi_1}{\partial y^2}\right) - \frac{1}{3}\left(\frac{\partial^2\psi_0}{\partial y^2}\right)^4\right\}\partial y = 0$$

$$\frac{\partial \theta_{10}}{\partial y} = 0 \text{ at } y = 0 \text{ and } B_h\,\theta_{10} + \frac{\partial \theta_{10}}{\partial y} = 0 \text{ at } y = h \tag{47}$$

The equation for the first order temperature expression along with convective boundary conditions is derived as

$$\frac{\partial \theta_{11}}{\partial y} + \theta_{00}\frac{\partial \theta_{10}}{\partial y} + \theta_{10}\frac{\partial \theta_{00}}{\partial y} = 0$$

$$\frac{\partial \theta_{11}}{\partial y} = 0 \text{ at } y = 0 \text{ and } B_h\,\theta_{11} + \frac{\partial \theta_{11}}{\partial y} = 0 \text{ at } y = h \tag{48}$$

By solving Eq. (45) - Eq. (48) and substituting in Eq. (27), the expression for temperature function is obtained as

i.e., $\theta = \theta_{00} + \nu\theta_{01} + A\,\theta_{10} + A\,\nu\,\theta_{11}$ (49)

Due to the complexity of the problem, solution for θ is obtained through MATLAB coding. The concentration solution can be obtained by applying the solution for θ to the solution of Eq. (11) in MATLAB programming.

3.1 Expression for Different Waveforms

The nondimensional expressions for sinusoidal, square, triangular, and trapezoidal wave forms are given as:

i. Sinusoidal wave:

$$h(x,t) = 1 + mx + \epsilon\,\text{Sin}\left[\frac{2\pi}{\lambda}(x - ct)\right]$$

ii. Square wave:

$$h(x,t) = 1 + mx + \epsilon\left[\frac{4}{\pi}\sum_{i=1}^{\infty}\frac{(-1)^{i+1}}{(2i-1)}\text{Cos}[(2i-1)2\pi(x-ct)]\right]$$

iii. Triangular wave:

$$h(x,t) = 1 + mx + \epsilon\left[\frac{8}{\pi^3}\sum_{i=1}^{\infty}\frac{(-1)^{i+1}}{(2i-1)^2}\text{Sin}[(2i-1)2\pi(x-ct)]\right]$$

iv. Trapezoidal wave

$$h(x,t) = 1 + mx + \epsilon\left[\frac{32}{\pi^2}\sum_{i=1}^{\infty}\frac{Sin\left(\frac{\pi}{8}\right)(2i-1)}{(2i-1)^2}\text{Sin}[(2i-1)2\pi(x-ct)]\right]$$

4. Graphical Analysis

Utilising the perturbation technique, the preceding section derived a semi-analytical solution for the heat and mass transfer of Eyring-Powell fluid characteristics in a non-uniform channel through which the fluid moves under varying conditions. The effects of varying fluid parameters are examined in this section. Table 1 illustrates the default values of physical parameters, MATLAB R2023a

provides graphical representations of physiological activity metrics along with flow quantities. Figures 2–12 further illustrate the effects of physiological factors on velocity, temperature, concentration, and bolus formation.

Table 1
Default values of physical parameters

Parameters	Default values taken	Range of values [34]
E_1	0.2	$0.01 \leq E_1 \leq 1$
E_2	0.2	$0.01 \leq E_2 \leq 1$
E_3	0.1	$0.1 \leq E_3 \leq 1$
E_4	0.001	$0.0 \leq E_4 \leq 1$
E_5	0.1	$0.0 \leq E_5 \leq 1$
Sc	0.5	$0.1 \leq Sc \leq 2$
Sr	0.5	$0.1 \leq Sr \leq 1.5$
Br	2	$0.1 \leq Br \leq 7$
B_h	1.5	$0 \leq B_h \leq 100$
B_m	1.5	$0 \leq B_m \leq 100$
A	0.01	$0 \leq A \leq 0.5$
B	2	$0 \leq B \leq 6$
t	0.1	$0.1 \leq t \leq 0.5$
x	0.2	$0 \leq x \leq 1.5$
Da	0.2	$0.01 \leq Da \leq 3$
β	0.2	$0 \leq x \leq 1.5$
ϵ	0.3	$0.1 \leq \epsilon \leq 1.5$
α	0.02	$\alpha \ll 1$
ν	0.02	$\nu \ll 1$
m	0.1	$0 \leq m \leq 1$

4.1 Flow Characteristics with Different Waveforms

Figure 2 - Figure 8 illustrate the impact of several key parameters on velocity profiles with different Waveforms. The waveforms are drawn to analyse the effectiveness and performance in various fluid dynamics applications, particularly in the blood flow in the cardiovascular system. The standard waveforms like Sinusoidal, Square, Triangular and Trapezoidal are drawn to analyse the effect of pertinent parameters on flow characteristics. The influence of the porosity parameter on fluid velocity is shown in Figure 2(a-d), which shows an improvement in velocity profiles when this parameter is increased. Higher porosity improves the fluid flow space, allowing for higher velocity. On the other hand, restricted permeability can raise fluid resistance and lower velocities. In Figure 3(a-d), the fluid flow decreases noticeably when the velocity slip parameter increases. Figure 4(a-d) shows the velocity connected with the Eyring-Powell Fluid Parameter A. It is evident that an increase in parameter A also results in an increase in velocity. In contrast, a decrease in velocity results from an increase in Eyring-Powell Fluid Parameter B, as seen in Figure 5(a-d). Figures 6(a-d) and 7(a-d) concentrate on the parameters α and m, that influence velocity profiles. Figure 6(a-d) reveals that the coefficient of variable viscosity improves velocity profiles, whereas Figure 7(a-d) illustrates the non-uniform parameter increases velocity profiles proportionally. The velocity profile is impacted by an increase in the degree of non-uniformity brought on by spatial differences in the fluid or channel geometry. The effects of wall tension, mass characterisation, wall-damping, rigidity, and elasticity parameters on velocity profiles are explored in detail (See Figure 8(a-d)). Increased wall tension and mass characterisation factors result in higher velocity profiles. On the other hand, velocity profiles decrease as the wall-damping value is increased. The wall rigidity and elasticity characteristics show similar effects. It can be noted from the figures that square waves have higher velocity when

compared to other waveforms. Trapezoidal waves also give better velocity profiles than triangular and sinusoidal waveforms.

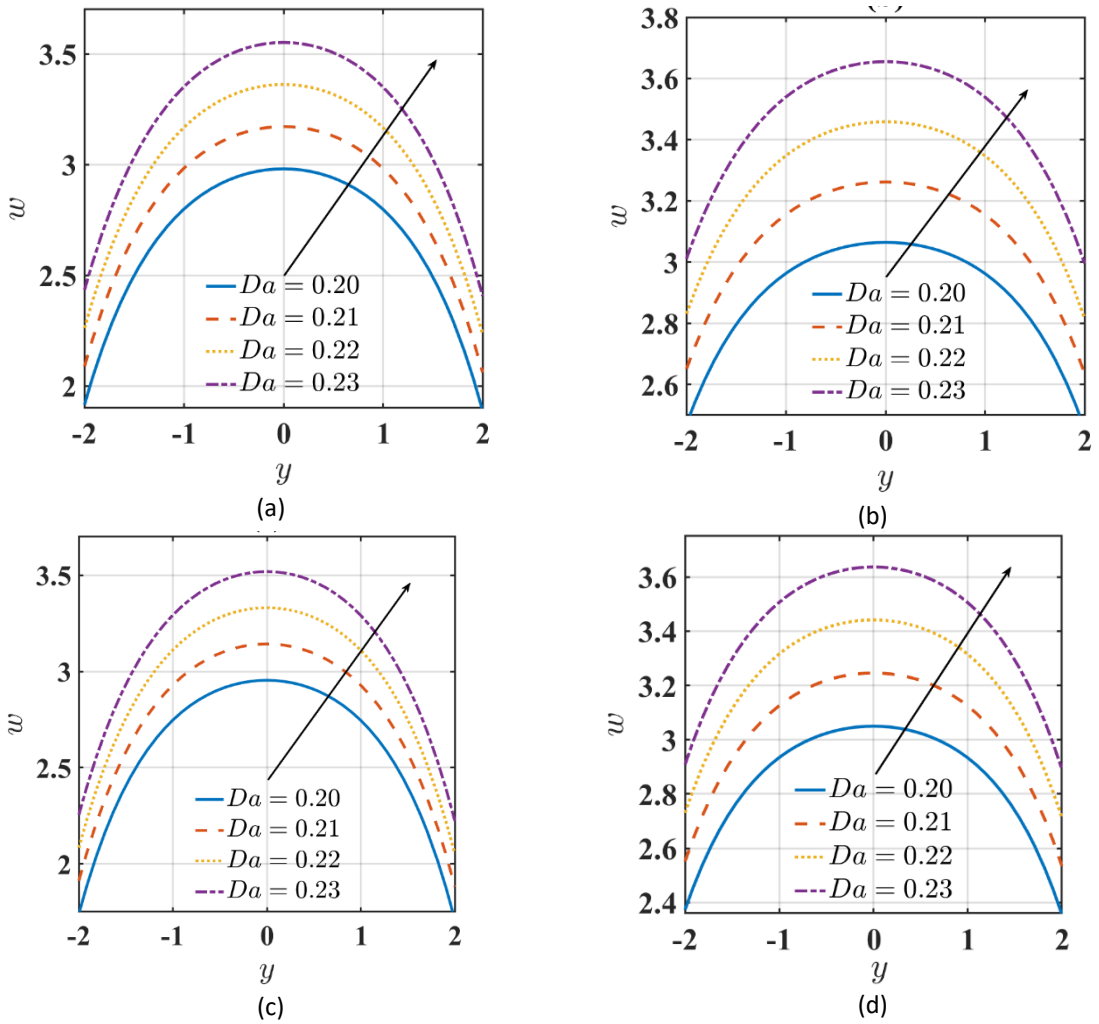

Fig. 2. Velocity Profile for variations in Darcy Number (Da) for different waveforms (a) Sinusoidal (b) Square (c) Triangular (d) Trapezoidal

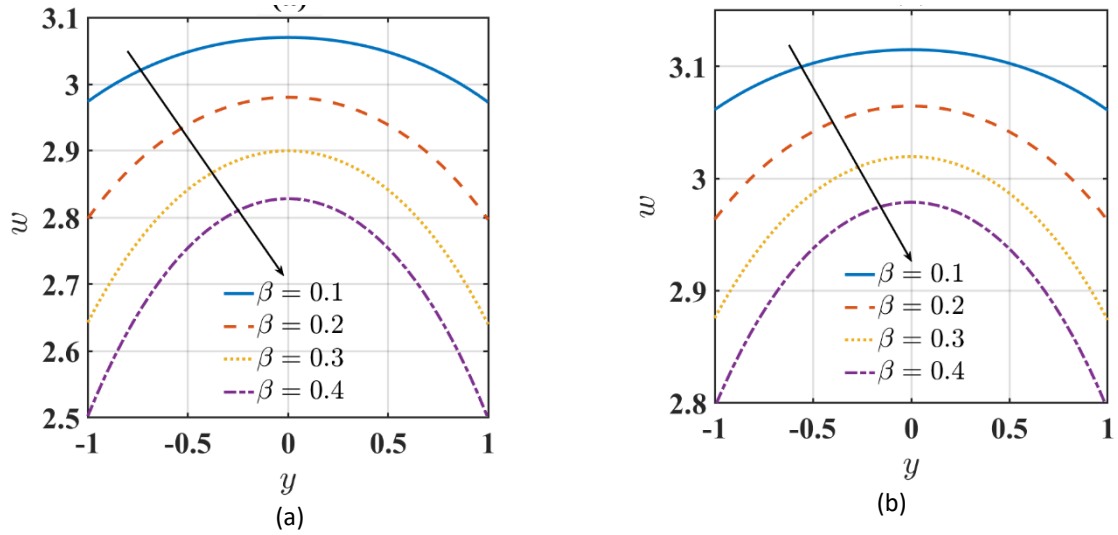

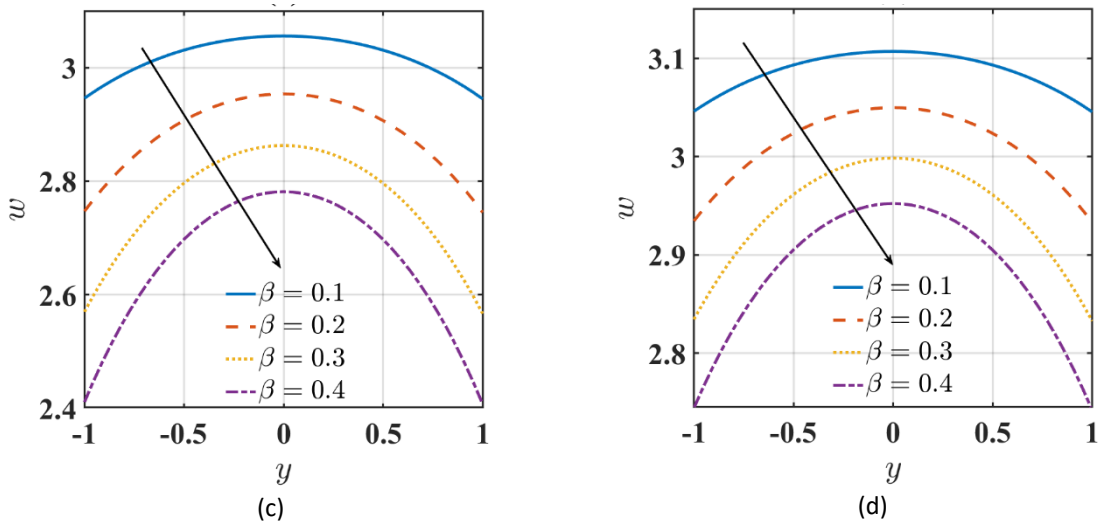

(c) (d)

Fig. 3. Velocity Profile for variations in velocity slip parameter (β) for different waveforms (a) Sinusoidal (b) Square (c) Triangular (d) Trapezoidal

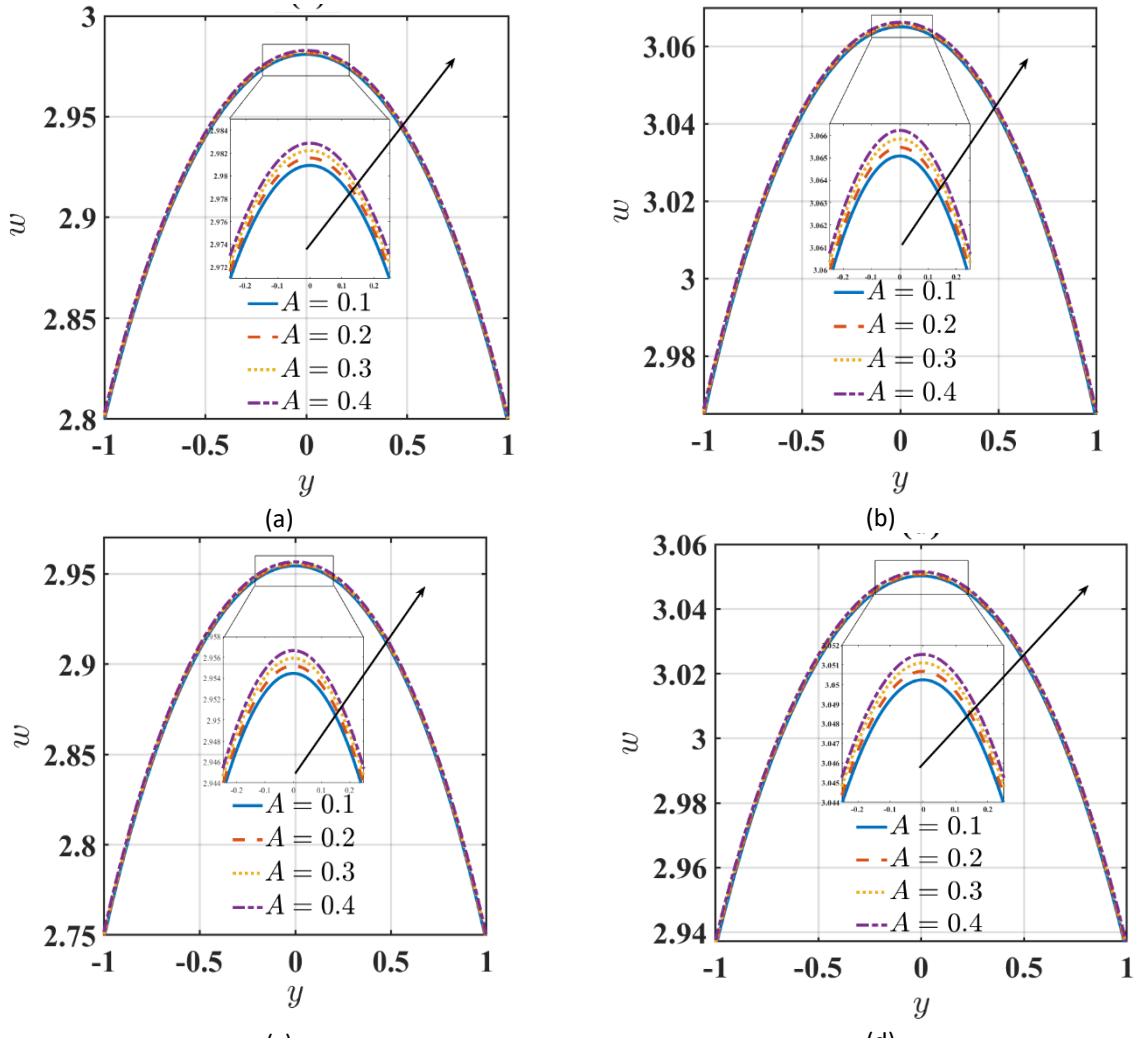

(a) (b)

(c) (d)

Fig. 4. Velocity Profile for variations in of Material parameter (A) for different waveforms (a) Sinusoidal (b) Square (c) Triangular (d) Trapezoidal

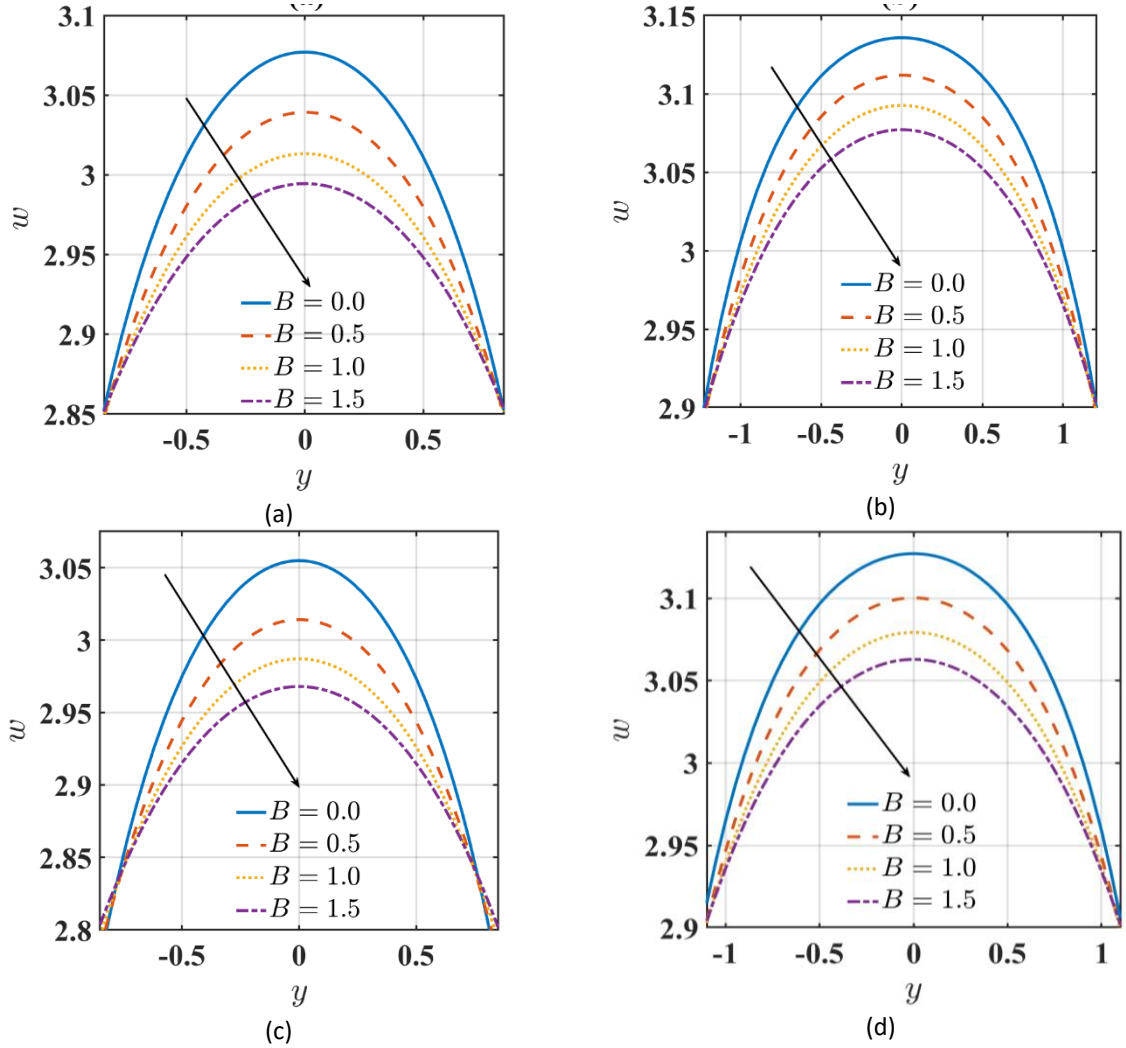

Fig. 5. Velocity Profile for variations in Material Parameter (B) for different waveforms (a) Sinusoidal (b) Square (c) Triangular (d) Trapezoidal

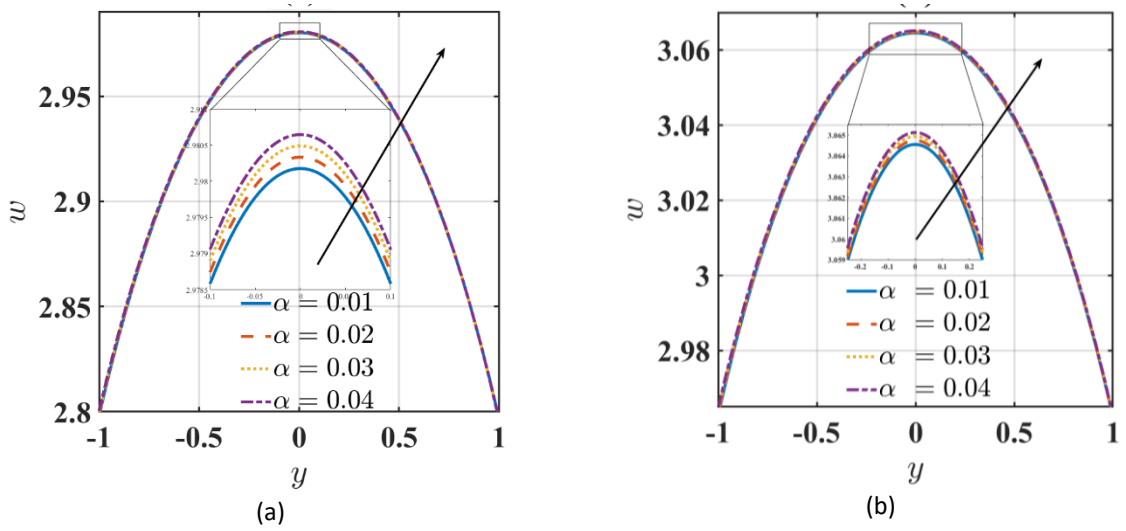

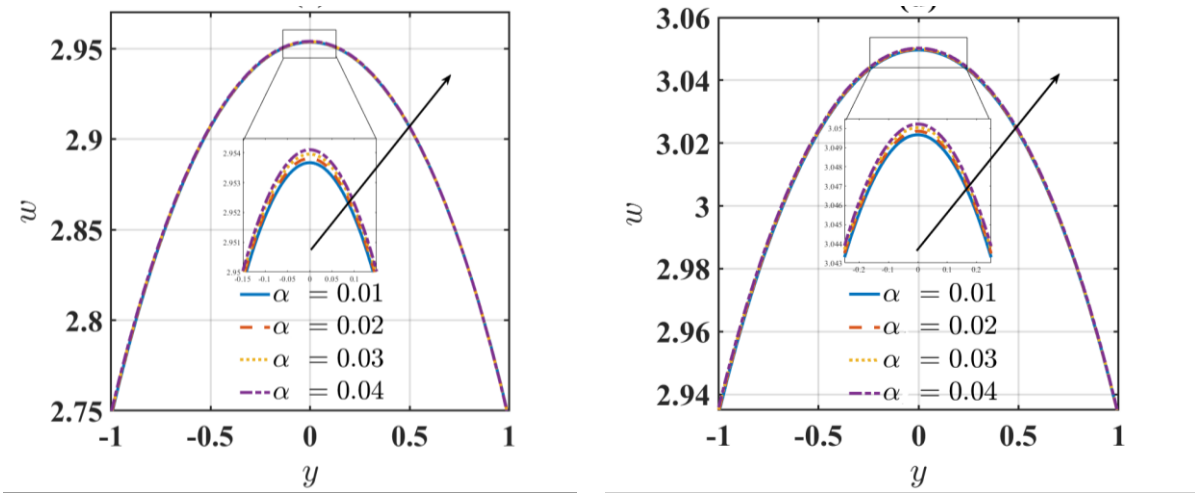

Fig. 6. Velocity Profile for variations in Coefficient of Variable Viscosity (α) for different waveforms (a) Sinusoidal (b) Square (c) Triangular (d) Trapezoidal

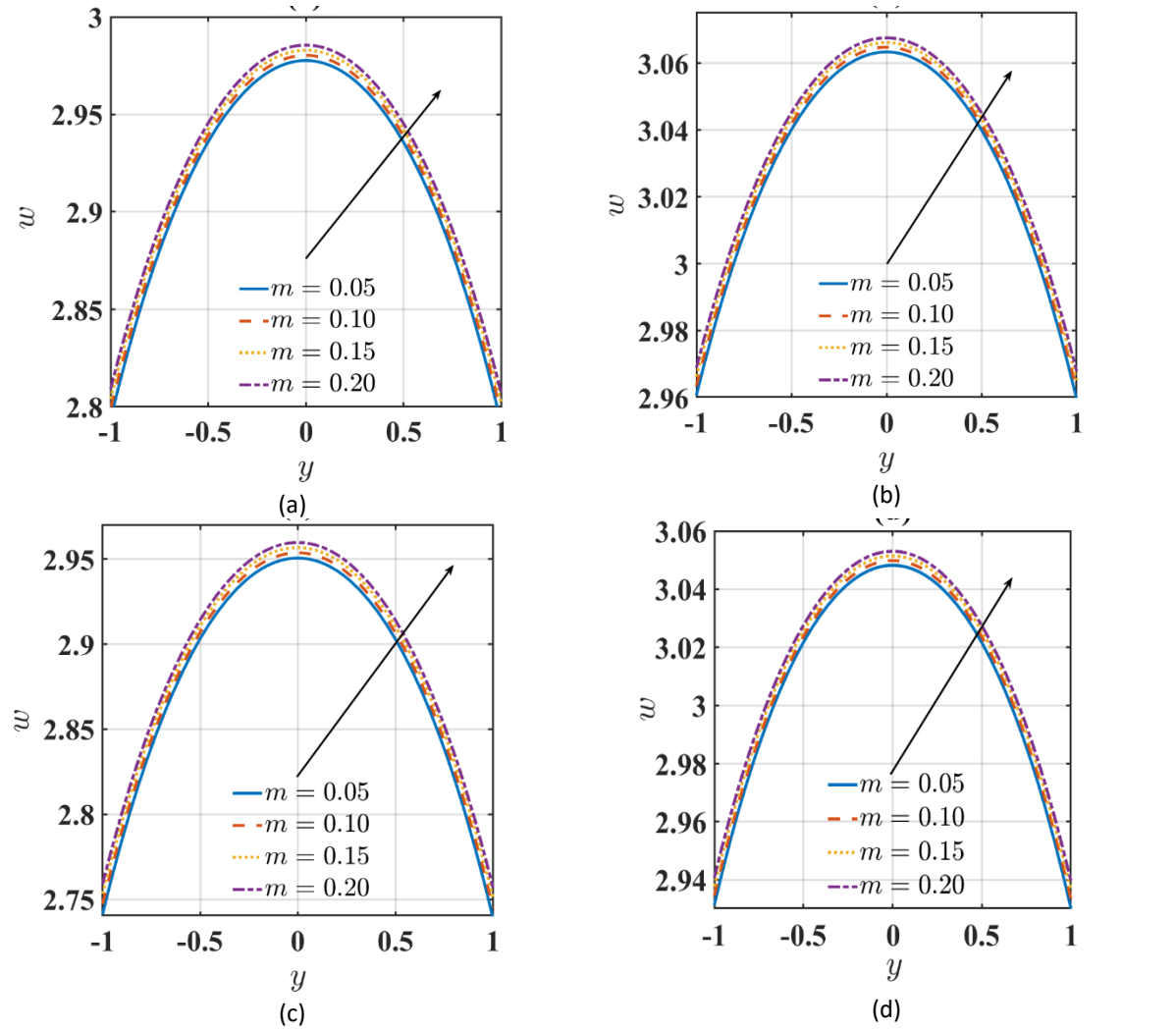

Fig. 7. Velocity Profile for variations in non-Uniform Parameter (m) for different waveforms (a) Sinusoidal (b) Square (c) Triangular (d) Trapezoidal

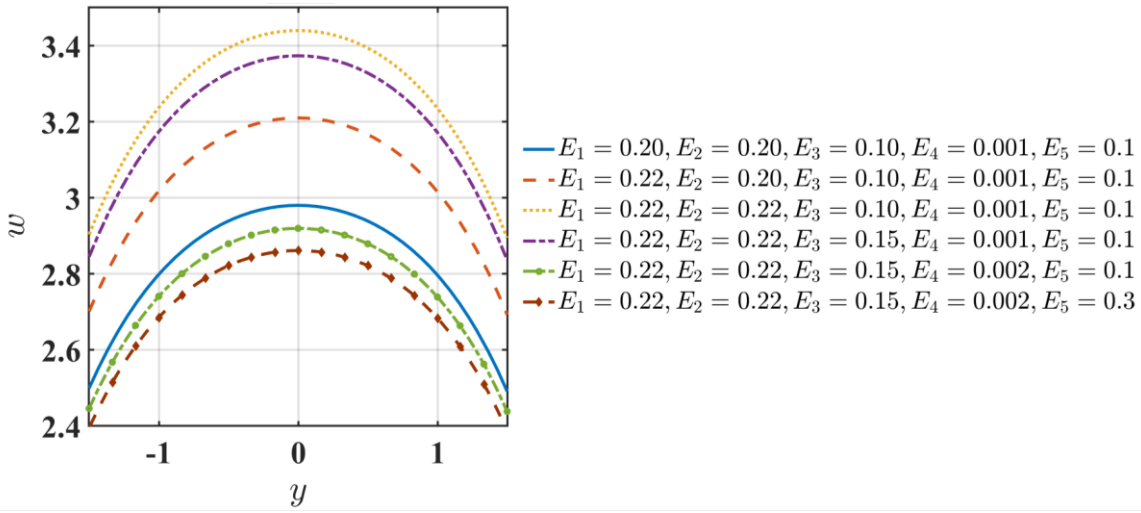
3.4
3.2
3
2.8
2.6
2.4
w
-1
0
1
y
$E_1 = 0.20, E_2 = 0.20, E_3 = 0.10, E_4 = 0.001, E_5 = 0.1$
$E_1 = 0.22, E_2 = 0.20, E_3 = 0.10, E_4 = 0.001, E_5 = 0.1$
$E_1 = 0.22, E_2 = 0.22, E_3 = 0.10, E_4 = 0.001, E_5 = 0.1$
$E_1 = 0.22, E_2 = 0.22, E_3 = 0.15, E_4 = 0.001, E_5 = 0.1$
$E_1 = 0.22, E_2 = 0.22, E_3 = 0.15, E_4 = 0.002, E_5 = 0.1$
$E_1 = 0.22, E_2 = 0.22, E_3 = 0.15, E_4 = 0.002, E_5 = 0.3$

(a)

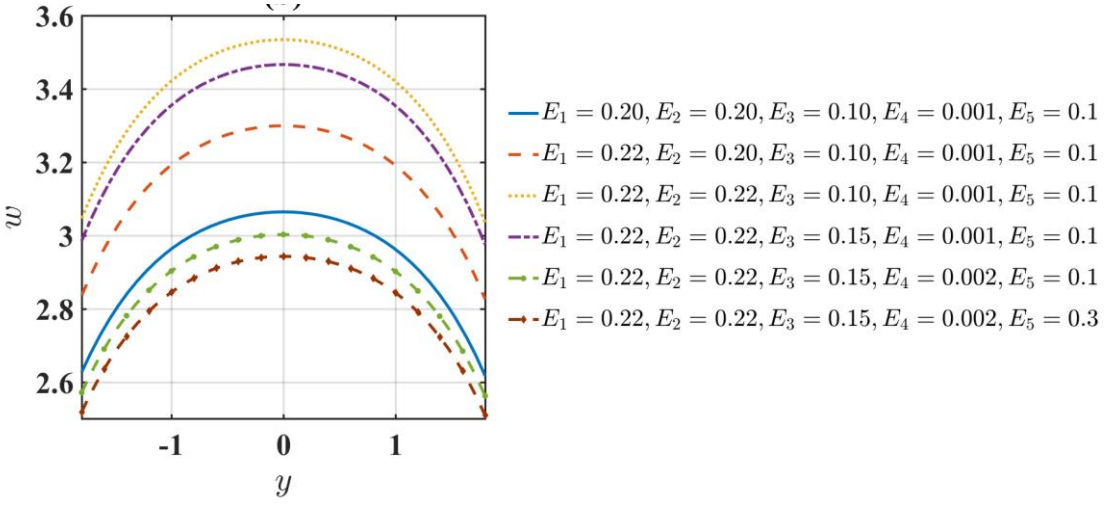
3.6
3.4
3.2
3
2.8
2.6
w
-1
0
1
y
$E_1 = 0.20, E_2 = 0.20, E_3 = 0.10, E_4 = 0.001, E_5 = 0.1$
$E_1 = 0.22, E_2 = 0.20, E_3 = 0.10, E_4 = 0.001, E_5 = 0.1$
$E_1 = 0.22, E_2 = 0.22, E_3 = 0.10, E_4 = 0.001, E_5 = 0.1$
$E_1 = 0.22, E_2 = 0.22, E_3 = 0.15, E_4 = 0.001, E_5 = 0.1$
$E_1 = 0.22, E_2 = 0.22, E_3 = 0.15, E_4 = 0.002, E_5 = 0.1$
$E_1 = 0.22, E_2 = 0.22, E_3 = 0.15, E_4 = 0.002, E_5 = 0.3$

(b)

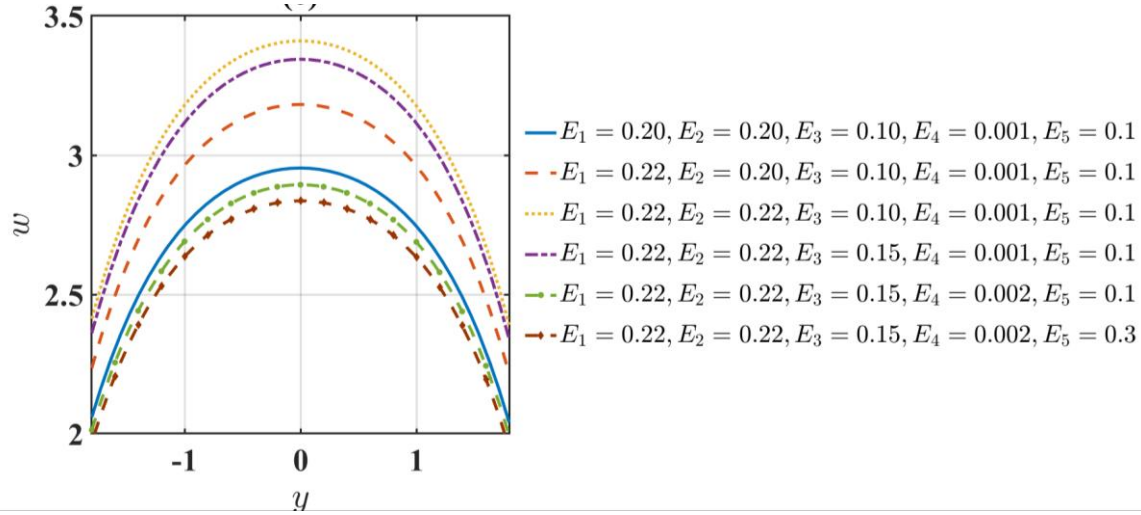
3.5
3
2.5
2
w
-1
0
1
y
$E_1 = 0.20, E_2 = 0.20, E_3 = 0.10, E_4 = 0.001, E_5 = 0.1$
$E_1 = 0.22, E_2 = 0.20, E_3 = 0.10, E_4 = 0.001, E_5 = 0.1$
$E_1 = 0.22, E_2 = 0.22, E_3 = 0.10, E_4 = 0.001, E_5 = 0.1$
$E_1 = 0.22, E_2 = 0.22, E_3 = 0.15, E_4 = 0.001, E_5 = 0.1$
$E_1 = 0.22, E_2 = 0.22, E_3 = 0.15, E_4 = 0.002, E_5 = 0.1$
$E_1 = 0.22, E_2 = 0.22, E_3 = 0.15, E_4 = 0.002, E_5 = 0.3$

(c)

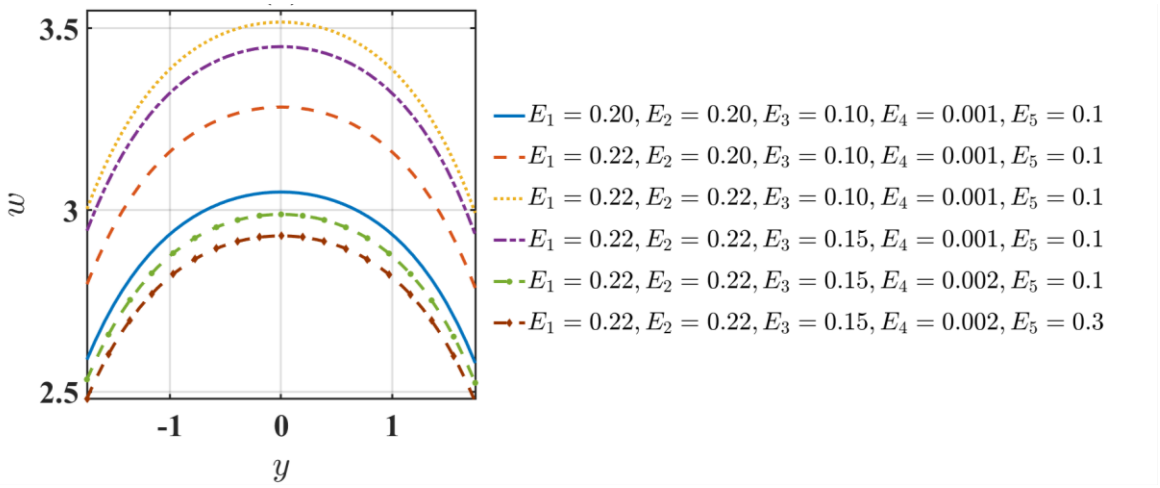

(d)

Fig. 8. Velocity Profile for variations in Wall Properties $(E_1 - E_5)$ for different waveforms (a) Sinusoidal (b) Square (c) Triangular (d) Trapezoidal

4.2 Heat Transfer Analysis

Figure 9(a) - Figure 9(g) are the graphical representations of temperature profiles, providing insight into the influence of numerous factors. Figure 9(a) and Figure 9(b) highlight the parameters Da and β. It is shown that temperature profiles and Da are directly correlated, and temperature profiles increase with a rise in the slip parameters. It is evident from Figure 9(c) that temperature profiles decrease as the material parameter B increases. There is a positive correlation between rising temperature profiles and increasing variable thermal conductivity, as shown in Figure 9(d). Temperature profiles show a decline with increasing convective heat transfer parameters (See Figure 9(e)). A notable temperature increase with an increase in the Brinkman number is seen in the drawing in Figure 9(f). With a greater Brinkman number, there may be an increase in fluid flow through the porous media. Increasing flow rates leads to higher temperatures due to viscous energy dissipation. Higher temperature profiles result from increased wall tension and mass characterisation, as seen in Figure 9(g). In contrast, when the wall-damping value increases, temperature profiles drop. Similar effects can be found for wall rigidity and elasticity parameters.

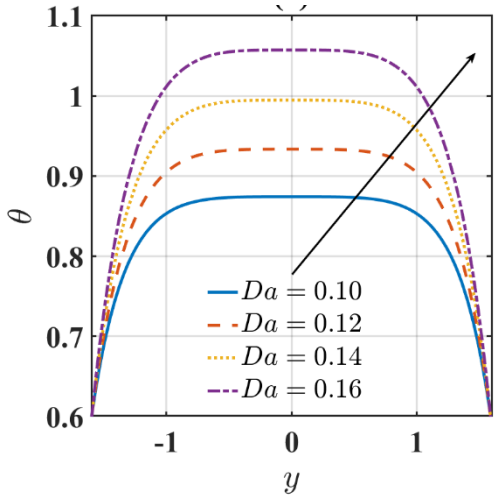

(a)

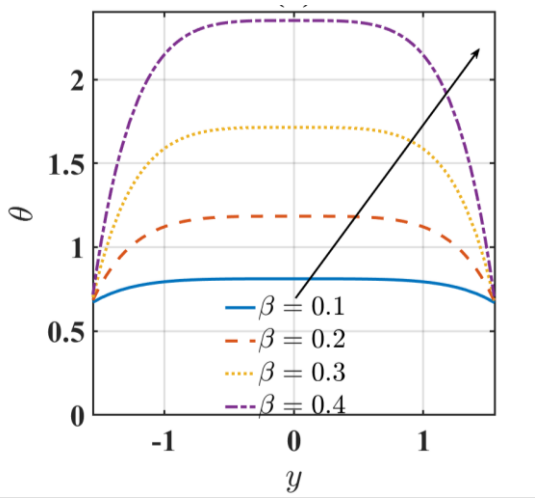

(b)

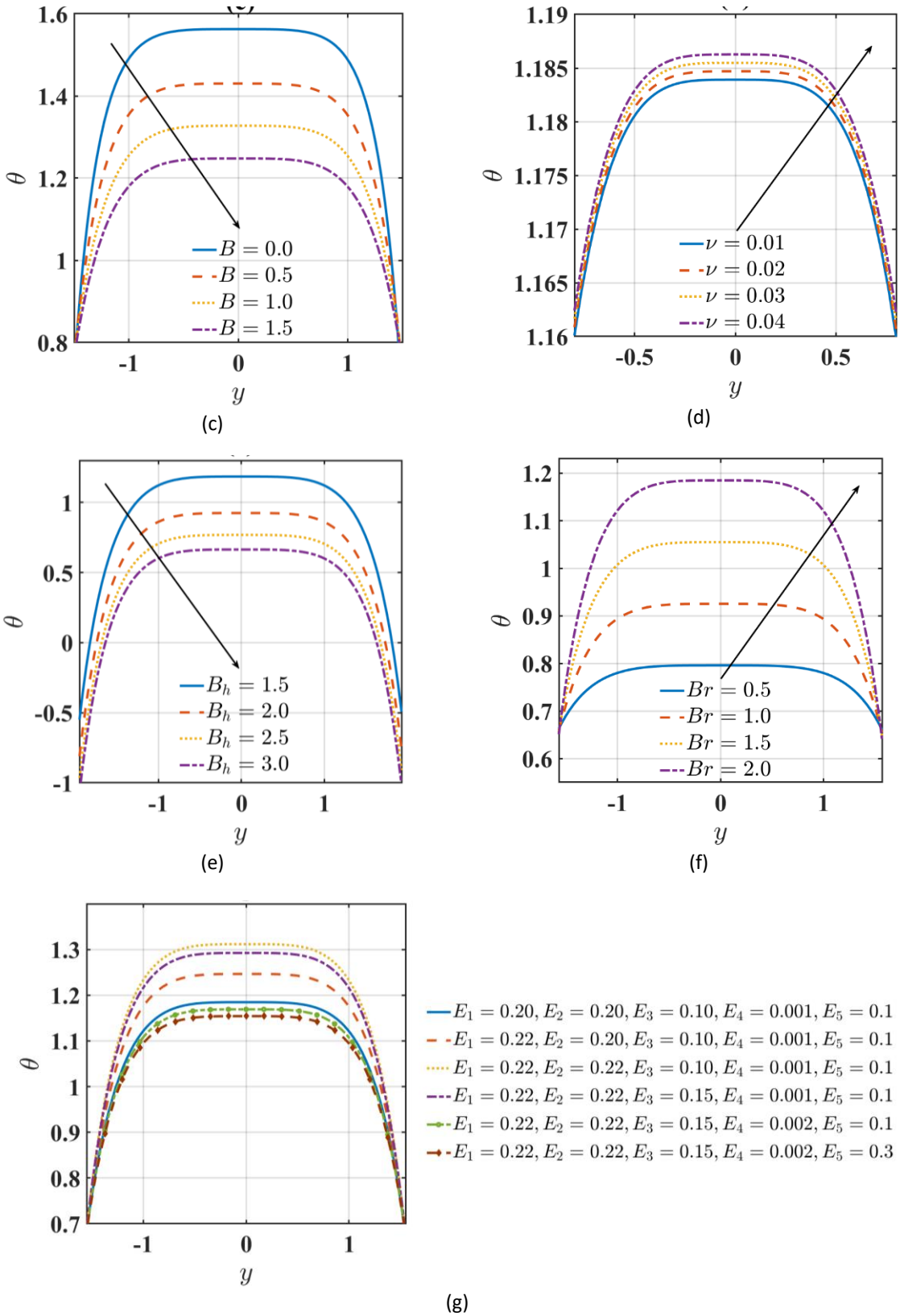

Fig. 9. Variation of temperature profiles for (a) Darcy Number (b) Velocity Slip Parameter (c) Material Parameter B (d) Variable Thermal Conductivity (e) Convective Heat Transfer Coefficient (f) Brickman Number (g) Wall Properties

4.3 Mass Transfer Analysis

Figure 10(a) - Figure 10(g) are intended to demonstrate the effect of critical parameters on concentration profiles. The lower concentration in Figure 10(a) is associated with a higher porous parameter. Figure 10(b) shows an opposite trend for material parameter B. Figure 10(c) and Figure 10(d) show varying effects for convective heat and mass transfer parameters, respectively. Increases in the convective heat parameter result in lower concentration profiles, whereas increases in the convective mass parameter result in higher concentration profiles. The variations in concentration profiles for Schmidt and Soret numbers are shown in Figure 10(e) and Figure 10(f), respectively. Greater Schmidt numbers restrict the mass transfer efficiency and may thin concentration boundary layers by decreasing concentration diffusion compared to momentum diffusion. Higher Soret numbers may result in reduced concentration gradients due to the greater influence of thermal processes on mass diffusion. Thus, as Schmidt and Soret numbers increase, concentration profiles decrease. Figure 10(g) shows that increased wall tension and mass characterisation result in reduced concentration profiles. On the other hand, concentration profiles are improved when the wall-damping value is raised. Similar effects are observed for wall rigidity and elasticity parameters.

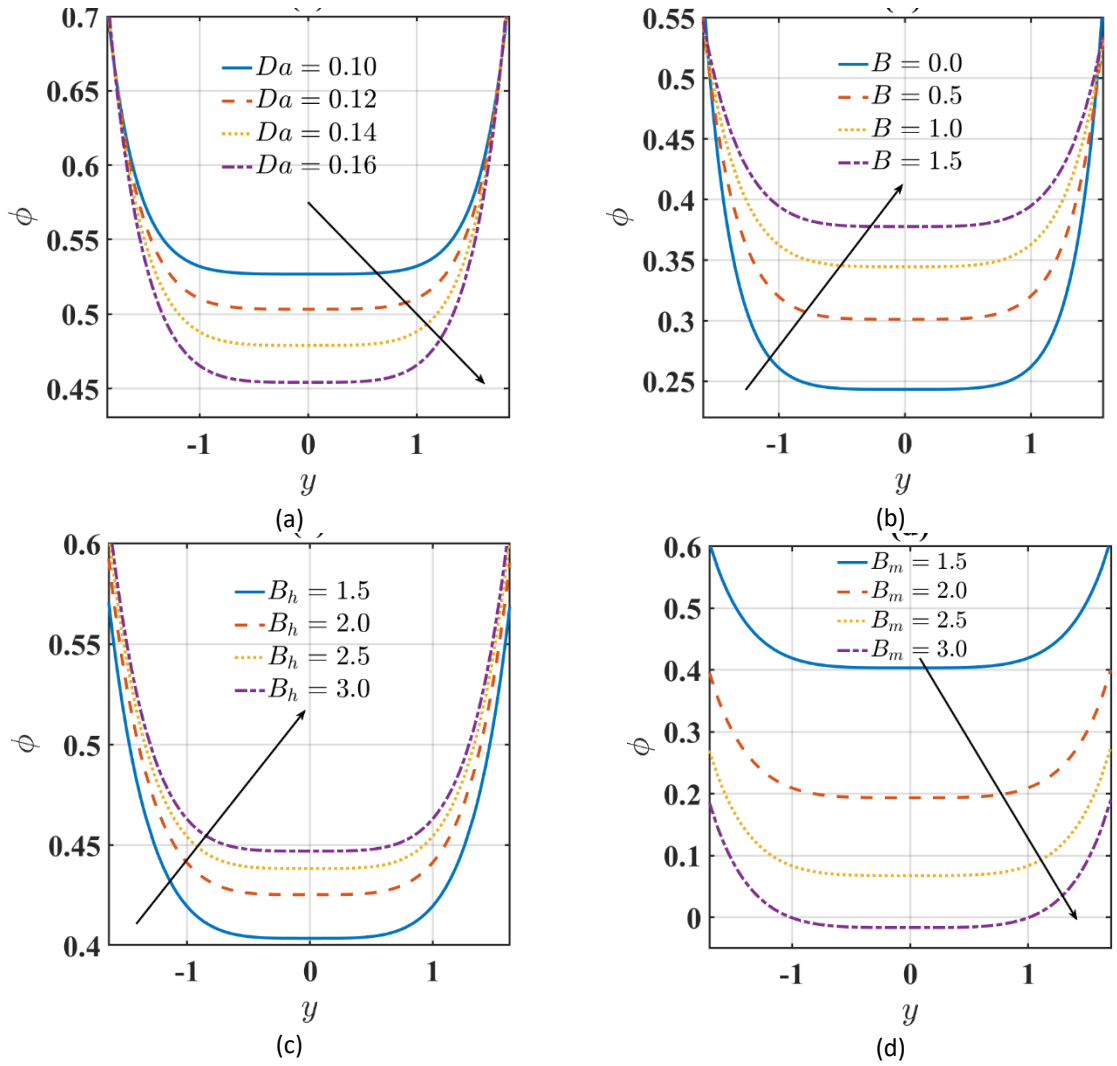

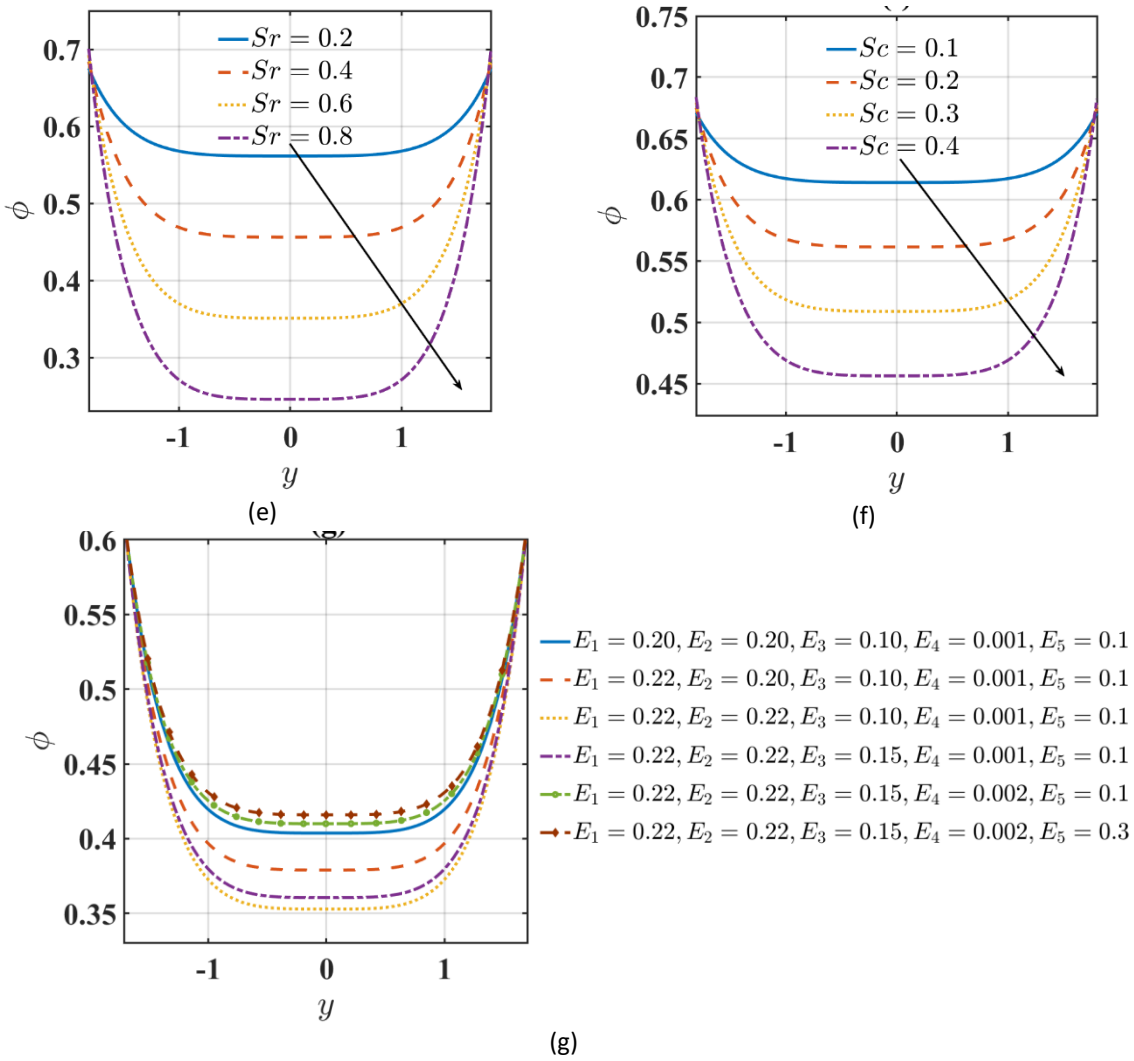

Fig. 10. Variation of Concentration profiles for (a) Darcy Number (b) Material Parameter B (c) Convective Heat Transfer Coefficient (d) Convective Mass Transfer Coefficient (e) Soret Number (f) Schmidt Number (g) Wall Properties

4.4 Trapping Phenomenon

The peristaltic trapping phenomenon includes temporarily confined biological fluids inside certain areas or structures while muscle contractions and relaxations propagate via tubular organs such as the digestive system. The trapping phenomenon is essential for a better understanding of fluid transport as it provides insight into the formation and movement of boluses, or tiny masses or material clusters, in constrained flow configurations. Figure 11 - Figure 14 show graphical representations and studies of many parameters impacting trapping during peristalsis. Figure 11 depicts different flow patterns corresponding to different values of the fluid parameter A, indicating a reduction in boluses as A increases. The fluid parameter B and bolus production have a reverse relationship in Figure 12, where an increase in B results in increased bolus formation. Figure 13 and Figure 14 examine the effects of parameters Da and β on trapped boluses, showing different effects on bolus production according to changes to the porosity and velocity slip parameters. From Figure 15, an increase in size of the bolus can be noted for a rise in non-uniform parameters.

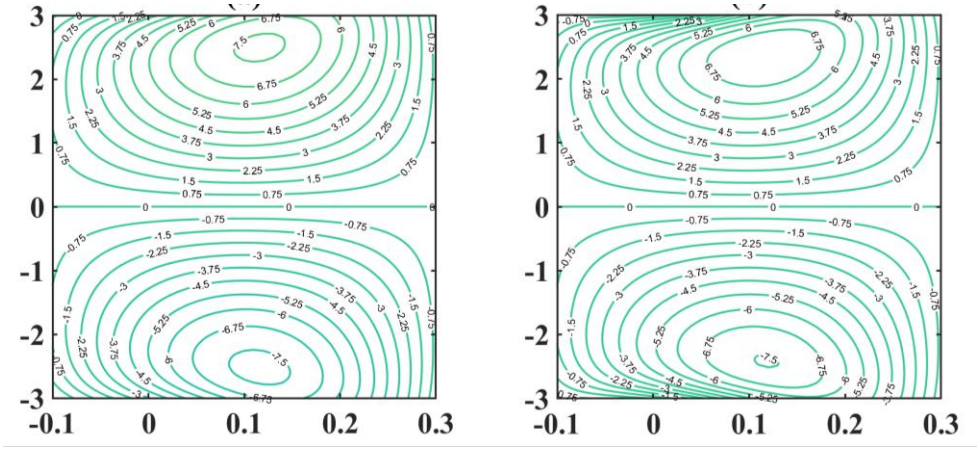

(a) (b)

Fig. 11. Variation of streamlines for (a) $A = 0.1$ and (b) $A = 0.4$

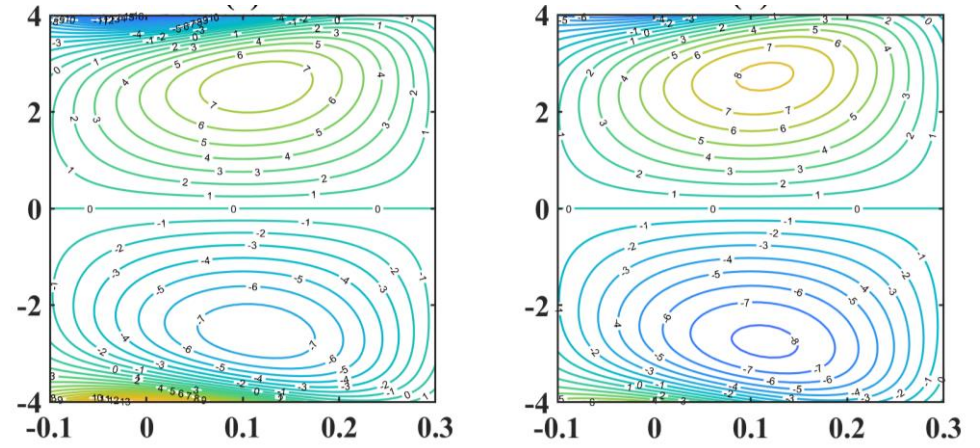

(a) (b)

Fig. 12. Variation of streamlines for (a) $B = 2.0$ and (b) $B = 2.5$

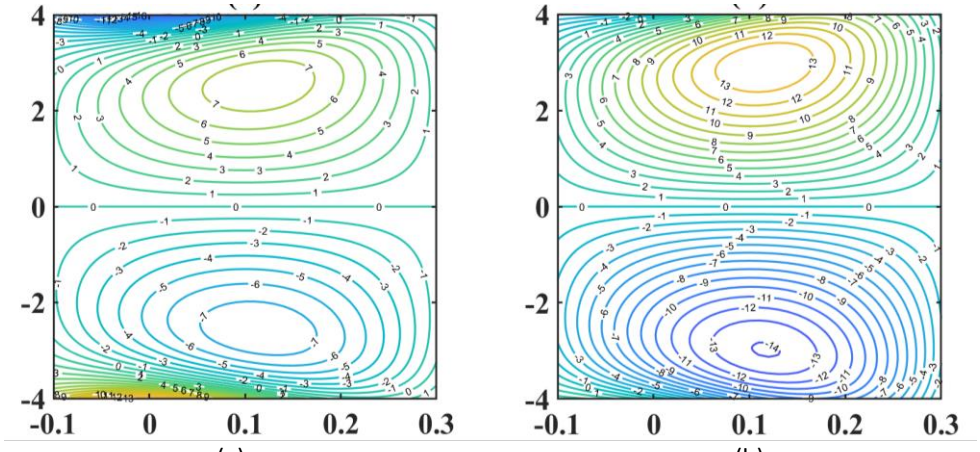

(a) (b)

Fig. 13. Variation of streamlines for (a) $Da = 0.1$ and (b) $Da = 0.2$

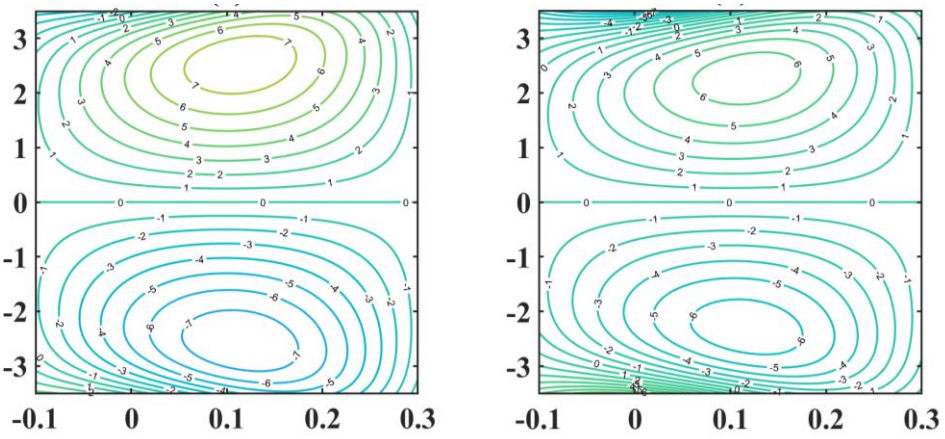

(a) (b)

Fig. 14. Variation of streamlines for (a) $\beta = 0.2$ and (b) $\beta = 0.3$

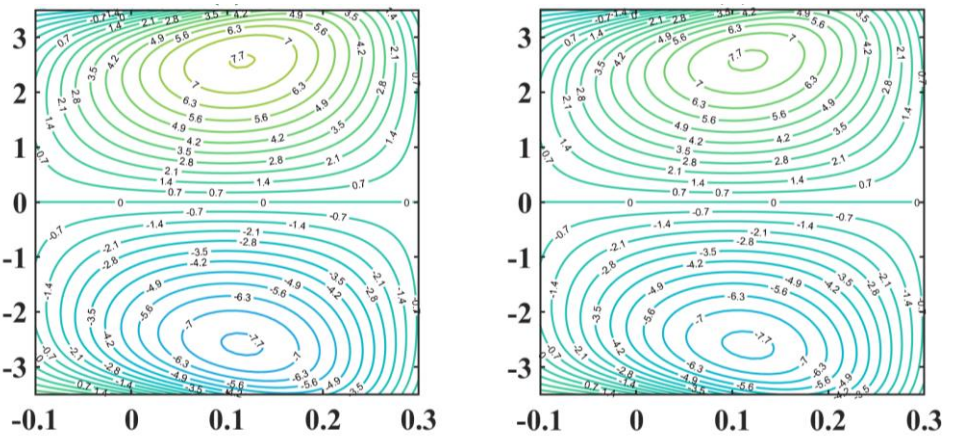

(a) (b)

Fig. 15. Variation of streamlines for (a) $m = 0.1$ and (b) $m = 0.2$

5. Validation of the Study

Elshehawey *et al.,* [4] investigate the peristaltic mechanism of Newtonian fluid through porous medium. Perturbation method is utilized to obtain the solution of axial velocity and pressure gradient component. The study also investigates the effect of frictional force on fluid flow. The present investigation involves the study of peristalsis of Eyring Powell fluid in a porous medium. Heat and Mass Transfer effect is investigated by considering porous and convective boundary conditions. Wall properties and variable liquid properties are also investigated. The current model is validated with the solution obtained for axial velocity in the study by Elshehawey *et al.,* [4] on setting fluid parameters $A = 0$ and $B = 0$, and coefficient of variable viscosity $\alpha = 0$. It has been noticed that the present study is in good agreement with Elshehawey *et al.,* [4].

6. Conclusion Remarks

The present mathematical methodology investigates the dynamics of peristaltic transport and Eyring-Powell fluids in porous media, thereby contributing significant theoretical understanding. Convective boundary conditions were incorporated into a non-uniform channel model to investigate these phenomena. Analyses of fluid motion were conducted by analysing velocity profiles of

trapezoidal, square, and triangular waveforms. The influence of fluctuations in various parameters on velocity, temperature, concentration, and streamlines are visually represented through graphs. The following is an overview of the model investigation:

i. Changes in embedding parameters, especially the Eyring-Powell fluid parameters, significantly impact the flow fields.
ii. Formation of bolus is impacted distinctly by velocity slip parameter and Darcy number variations.
iii. Enhancement of the Convective Heat Transfer Coefficient reduces the temperature field, whereas rising slip parameter and Darcy numbers increases.
iv. Square Waves gives better velocity profile than other waveforms.
v. In numerous instances, considering increasing Soret and Schmidt numbers leads to a reduction in concentration profiles.
vi. Damping force parameter increases the temperature profiles, although wall tension and mass characterization parameters does not vary. This state impacts various biological and physiological systems and is crucial to system thermodynamics.
vii. An increase in porosity results in an improvement in fluid flow space, which in turn leads to an increase in velocity profiles.

This model focuses on the peristaltic flow of Eyring-Powell Fluid with Variable fluid properties. The study considered the viscosity varying with the thickness of the fluid layers. This study can be extended by considering variable viscosity with respect to temperature. The study can also be extended by considering slip boundary conditions as it has many biological importance.

References

[1] AYUKAWA, Kyozo, and Shin TAKABATAKE. "Numerical Analysis of Two-Dimensional Peristaltic Flows: 1st Report, Flow Pattern." *Bulletin of JSME* 25, no. 205 (1982): 1061-1069. https://doi.org/10.1299/jsme1958.25.1061
[2] Siddiqui, A. M., and W. H. Schwarz. "Peristaltic flow of a second-order fluid in tubes." *Journal of Non-Newtonian Fluid Mechanics* 53 (1994): 257-284. https://doi.org/10.1016/0377-0257(94)85052-6
[3] Comparini, Elena, and Paola Mannucci. "Flow of a Bingham fluid in contact with a Newtonian fluid." *Journal of mathematical analysis and applications* 227, no. 2 (1998): 359-381. https://doi.org/10.1006/jmaa.1998.6098
[4] Elshehawey, Elsayed F., Ayman MF Sobh, and Elsayed ME Elbarbary. "Peristaltic motion of a generalized Newtonian fluid through a porous medium." *Journal of the Physical Society of Japan* 69, no. 2 (2000): 401-407. https://doi.org/10.1143/JPSJ.69.401
[5] Hayat, T., F. M. Mahomed, and S. Asghar. "Peristaltic flow of a magnetohydrodynamic Johnson–Segalman fluid." *Nonlinear Dynamics* 40 (2005): 375-385. https://doi.org/10.1007/s11071-005-7799-0
[6] Srinivas, S., R. Gayathri, and M. Kothandapani. "The influence of slip conditions, wall properties and heat transfer on MHD peristaltic transport." *Computer physics communications* 180, no. 11 (2009): 2115-2122. https://doi.org/10.1016/j.cpc.2009.06.015
[7] Ramesh, K., and M. Devakar. "Magnetohydrodynamic peristaltic transport of couple stress fluid through porous medium in an inclined asymmetric channel with heat transfer." *Journal of Magnetism and Magnetic Materials* 394 (2015): 335-348. https://doi.org/10.1016/j.jmmm.2015.06.052
[8] Sankad, G. C., and Pratima S. Nagathan. "Unsteady MHD peristaltic flow of a couple stress fluid through porous medium with wall and slip effects." *Alexandria Engineering Journal* 55, no. 3 (2016): 2099-2105. https://doi.org/10.1016/j.aej.2016.06.029
[9] Gudekote, Manjunatha, and Rajashekhar Choudhari. "Slip effects on peristaltic transport of Casson fluid in an inclined elastic tube with porous walls." *Journal of Advanced Research in Fluid Mechanics and Thermal Sciences* 43, no. 1 (2018): 67-80.
[10] Lakshminarayana, Pallavarapu, K. Vajravelu, G. Sucharitha, and S. Sreenadh. "Peristaltic slip flow of a Bingham fluid in an inclined porous conduit with Joule heating." *Applied Mathematics and Nonlinear Sciences* 3, no. 1 (2018): 41-54. https://doi.org/10.21042/AMNS.2018.1.00005

[11] Vaidya, Hanumesh, C. Rajashekhar, G. Manjunatha, K. V. Prasad, O. D. Makinde, and K. Vajravelu. "Heat and mass transfer analysis of MHD peristaltic flow through a complaint porous channel with variable thermal conductivity." *Physica Scripta* 95, no. 4 (2020): 045219.

[12] Tanveer, A., and Muhammad Yousaf Malik. "Slip and porosity effects on peristalsis of MHD Ree-Eyring nanofluid in curved geometry." *Ain Shams Engineering Journal* 12, no. 1 (2021): 955-968. https://doi.org/10.1016/j.asej.2020.04.008

[13] Abuiyada, Alaa, Nabil Eldabe, Mohamed Abouzeid, and Samy Elshaboury. "Influence of Both Ohmic Dissipation and Activation Energy on Peristaltic Transport of Jeffery Nanofluid through a Porous Media." *CFD Letters* 15, no. 6 (2023): 65-85. https://doi.org/10.37934/cfdl.15.6.6585

[14] Pascal, J. P., N. Gonputh, and S. J. D. D'Alessio. "Long-wave instability of flow with temperature dependent fluid properties down a heated incline." *International Journal of Engineering Science* 70 (2013): 73-90. https://doi.org/10.1016/j.ijengsci.2013.05.003

[15] Latif, T., N. Alvi, Q. Hussain, and S. Asghar. "Variable properties of MHD third order fluid with peristalsis." *Results in physics* 6 (2016): 963-972. https://doi.org/10.1016/j.rinp.2016.11.016

[16] Khan, Mair, T. Salahuddin, and M. Y. Malik. "An immediate change in viscosity of Carreau nanofluid due to double stratified medium: application of Fourier's and Fick's laws." *Journal of the Brazilian Society of Mechanical Sciences and Engineering* 40 (2018): 1-10. https://doi.org/10.1007/s40430-018-1371-6

[17] Khan, Mair, T. Salahuddin, M. Y. Malik, and Fouad Othman Mallawi. "Change in viscosity of Williamson nanofluid flow due to thermal and solutal stratification." *International Journal of Heat and Mass Transfer* 126 (2018): 941-948. https://doi.org/10.1016/j.ijheatmasstransfer.2018.05.074

[18] Manjunatha, G., C. Rajashekhar, Hanumesh Vaidya, K. V. Prasad, O. D. Makinde, and J. U. Viharika. "Impact of variable transport properties and slip effects on MHD Jeffrey fluid flow through channel." *Arabian Journal for Science and Engineering* 45 (2020): 417-428. https://doi.org/10.1007/s13369-019-04266-y

[19] Khan, Waqar Azeem, Shahid Farooq, S. Kadry, M. Hanif, F. J. Iftikhar, and Syed Zaheer Abbas. "Variable characteristics of viscosity and thermal conductivity in peristalsis of magneto-Carreau nanoliquid with heat transfer irreversibilities." *Computer Methods and Programs in Biomedicine* 190 (2020): 105355. https://doi.org/10.1016/j.cmpb.2020.105355

[20] Prasad, K. V., Hanumesh Vaidya, C. Rajashekhar, Sami Ullah Khan, G. Manjunatha, and J. U. Viharika. "Slip flow of MHD Casson fluid in an inclined channel with variable transport properties." *Communications in Theoretical Physics* 72, no. 9 (2020): 095004. 10.1088/1572-9494/aba246

[21] Mukhopadhyay, Anandamoy, Souradip Chattopadhyay, and Amlan K. Barua. "Effects of strong viscosity with variable fluid properties on falling film instability." In *Advances in Nonlinear Dynamics: Proceedings of the Second International Nonlinear Dynamics Conference (NODYCON 2021), Volume 1*, pp. 75-85. Cham: Springer International Publishing, 2021. https://doi.org/10.1007/978-3-030-81162-4_7

[22] Vajravelu, K., S. Sreenadh, and P. Lakshminarayana. "The influence of heat transfer on peristaltic transport of a Jeffrey fluid in a vertical porous stratum." *Communications in Nonlinear Science and Numerical Simulation* 16, no. 8 (2011): 3107-3125. https://doi.org/10.1016/j.cnsns.2010.11.001

[23] Alarabi, Tagreed, Assma F. Elsayed, and O. Anwar Bég. "Homotopy perturbation method for heat transfer in peristaltic flow of viscoelastic fluid in an eccentric cylinder with variable effects." *Life Science Journal* 11, no. 7 (2014): 197-206.

[24] Dar, Ajaz Ahmad, and K. Elangovan. "Influence of an inclined magnetic field on heat and mass transfer of the peristaltic flow of a couple stress fluid in an inclined channel." *World Journal of Engineering* 14, no. 1 (2017): 7-18. https://doi.org/10.1108/WJE-11-2016-0124

[25] Abdulhadi, Ahmed M., and Tamara S. Ahmed. "Effect of radial magnetic field on peristaltic transport of Jeffrey fluid in curved channel with heat/mass transfer." In *Journal of Physics: Conference Series*, vol. 1003, no. 1, p. 012053. IOP Publishing, 2018. 10.1088/1742-6596/1003/1/012053

[26] Khan, Mair, M. Y. Malik, T. Salahuddin, and Arif Hussian. "Heat and mass transfer of Williamson nanofluid flow yield by an inclined Lorentz force over a nonlinear stretching sheet." *Results in Physics* 8 (2018): 862-868. https://doi.org/10.1016/j.rinp.2018.01.005

[27] Magesh, A., and M. Kothandapani. "Heat and mass transfer analysis on non-Newtonian fluid motion driven by peristaltic pumping in an asymmetric curved channel." *The European Physical Journal Special Topics* 230, no. 5 (2021): 1447-1464. https://doi.org/10.1140/epjs/s11734-021-00035-x

[28] Vaidya, Hanumesh, C. Rajashekhar, Manjunatha Gudekote, and K. V. Prasad. "Heat transfer and slip consequences on peristaltic transport of a casson fluid in an axisymmetric porous tube." *Journal of Porous Media* 24, no. 3 (2021). 10.1615/JPorMedia.2021025262

[29] Hayat, T., Anum Tanveer, Humaira Yasmin, and Fuad Alsaadi. "Simultaneous effects of Hall current and thermal deposition in peristaltic transport of Eyring–Powell fluid." *International Journal of Biomathematics* 8, no. 02 (2015): 1550024. https://doi.org/10.1142/S1793524515500242

[30] Akbar, Noreen Sher. "Application of Eyring-Powell fluid model in peristalsis with nano particles." *Journal of Computational and Theoretical Nanoscience* 12, no. 1 (2015): 94-100. https://doi.org/10.1166/jctn.2015.3703

[31] Hina, S. "MHD peristaltic transport of Eyring–Powell fluid with heat/mass transfer, wall properties and slip conditions." *Journal of Magnetism and Magnetic Materials* 404 (2016): 148-158. https://doi.org/10.1016/j.jmmm.2015.11.059

[32] Riaz, Arshad. "Thermal analysis of an Eyring–Powell fluid peristaltic transport in a rectangular duct with mass transfer." *Journal of Thermal Analysis and Calorimetry* 143 (2021): 2329-2341. https://doi.org/10.1007/s10973-020-09723-7

[33] Irfan, M., W. A. Khan, Amjad Ali Pasha, Mohammad Irfan Alam, Nazrul Islam, and M. Zubair. "Significance of non-Fourier heat flux on ferromagnetic Powell-Eyring fluid subject to cubic autocatalysis kind of chemical reaction." *International Communications in Heat and Mass Transfer* 138 (2022): 106374. https://doi.org/10.1016/j.icheatmasstransfer.2022.106374

[34] Anjum, Nazash, W. A. Khan, A. Hobiny, M. Azam, M. Waqas, and M. Irfan. "Numerical analysis for thermal performance of modified Eyring Powell nanofluid flow subject to activation energy and bioconvection dynamic." *Case Studies in Thermal Engineering* 39 (2022): 102427. https://doi.org/10.1016/j.csite.2022.102427

[35] Bhattacharyya, A., R. Kumar, S. Bahadur, and G. S. Seth. "Modeling and interpretation of peristaltic transport of Eyring–Powell fluid through uniform/non-uniform channel with Joule heating and wall flexibility." *Chinese Journal of Physics* 80 (2022): 167-182. https://doi.org/10.1016/j.cjph.2022.06.018

[36] Gudekote, Manjunatha, Rajashekhar Choudhari, Prathiksha Sanil, Hanumesh Vaidya, Balachandra Hadimani, Kerehalli Vinayaka Prasad, and Jyoti Shetty. "Impact of Variable Liquid Properties on Peristaltic Transport of Non-Newtonian Fluid Through a Complaint Non-Uniform Channel." *Journal of Advanced Research in Fluid Mechanics and Thermal Sciences* 103, no. 2 (2023): 20-39. https://doi.org/10.37934/arfmts.103.2.2039

[37] Hadimani, Balachandra, Rajashekhar Choudhari, Prathiksha Sanil, Hanumesh Vaidya, Manjunatha Gudekote, Kerehalli Vinayaka Prasad, and Jyoti Shetty. "The Influence of Variable Fluid Properties on Peristaltic Transport of Eyring Powell Fluid Flowing Through an Inclined Uniform Channel." *Journal of Advanced Research in Fluid Mechanics and Thermal Sciences* 102, no. 2 (2023): 166-185. https://doi.org/10.37934/arfmts.102.2.166185

[38] Boujelbene, Mohamed, Balachandra Hadimani, Rajashekhar Choudhari, Prathiksha Sanil, Manjunatha Gudekote, Hanumesh Vaidya, Kerehalli Vinayaka Prasad *et al.,* "Impact of Variable Slip and Wall Properties on Peristaltic Flow of Eyring–Powell Fluid Through Inclined Channel: Artificial Intelligence Based Perturbation Technique." *Fractals* 31, no. 06 (2023): 2340140. https://doi.org/10.1142/S0218348X23401400

[39] Khan, Waqar Azeem. "Dynamics of gyrotactic microorganisms for modified Eyring Powell nanofluid flow with bioconvection and nonlinear radiation aspects." *Waves in Random and Complex Media* (2023): 1-11. https://doi.org/10.1080/17455030.2023.2168086